https://doi.org/10.5194/egusphere-2024-401
Preprint. Discussion started: 13 February 2024

Global modeling of aerosol nucleation with an explicit chemical mechanism for highly oxygenated organic molecules (HOMs)

Xinyue Shao[1,2], Minghuai Wang[1,2], Xinyi Dong[1,2], Yaman Liu[1,3], Wenxiang Shen[1,2], Stephen R. Arnold[4], Leighton A. Regayre[4,5,6], Meinrat O. Andreae[7,8], Mira L. Pöhlker[7,9,10], Duseong S. Jo[11], Yue Man[1,3], and Ken S. Carslaw[4]

[1]School of Atmospheric Science, Nanjing University, Nanjing, 210023, China
[2]Joint International Research Laboratory of Atmospheric and Earth System Sciences & Institute for Climate and Global Change Research, Nanjing University, Nanjing, 210023, China
[3]Zhejiang Institute of Meteorological Sciences, Hangzhou, 310008, China
[4]Institute for Climate and Atmospheric Science, School of Earth and Environment, University of Leeds, Leeds, LS2 9JT, UK
[5]Met Office Hadley Centre, Exeter, Fitzroy Road, Exeter, Devon, EX1 3PB, UK
[6]Centre for Environmental Modelling and Computation, School of Earth and Environment, University of Leeds, Leeds, LS2 9JT, UK
[7]Max Planck Institute for Chemistry, Mainz, 55020, Germany
[8]Scripps Institution of Oceanography, University of California San Diego, La Jolla, USA
[9]Leipzig Institute for Meteorology, Universität Leipzig, 04103 Leipzig, Germany
[10]Experimental Aerosol and Cloud Microphysics Department, Leibniz Institute for Tropospheric Research, 04318 Leipzig, Germany
[11]Atmospheric Chemistry Observations and Modeling Laboratory, National Center for Atmospheric Research, Boulder, CO 80103, USA

Correspondence to: Minghuai Wang (minghuai.wang@nju.edu.cn), Xinyi Dong (dongxy@nju.edu.cn)

Abstract. New particle formation (NPF) involving organic compounds has been identified as an important process affecting aerosol particle number concentrations in the global atmosphere. Laboratory studies have shown that highly oxygenated organic molecules (HOMs) can make a substantial contribution to NPF, but there is a lack of global model studies of NPF with detailed HOMs chemistry. Here, we add a state-of-art biogenic HOMs chemistry scheme with 96 chemical reactions to a global chemistry-climate model and quantify the contribution to global aerosols through HOMs-driven NPF. The updated model captures the frequency of NPF events observed at continental surface sites (normalized mean bias changes from -96% to -15%) and shows reasonable agreement with measured rates of NPF and sub-20nm particle growth. Sensitivity simulations show that the effect of HOMs on particle growth is more important for particle number than the effect on particle formation. Globally, organics contribute around 45% of the annual mean vertically-integrated nucleation rate (at 1nm) and 25% of the vertically-averaged growth rate. The inclusion of HOMs-related processes leads to a 39% increase in the global annual mean aerosol number burden and a 33% increase in cloud condensation nuclei (CCN) burden at 0.5% supersaturation compared to

https://doi.org/10.5194/egusphere-2024-401
Preprint. Discussion started: 13 February 2024

a simulation with only inorganic nucleation. Our work predicts a greater contribution of organic nucleation to NPF than previous studies due to the explicit HOMs mechanism and an updated inorganic NPF scheme. The large contribution of biogenic HOMs to NPF on a global scale could make global aerosol sensitive to changes in biogenic emissions.

1 Introduction

Aerosol particles exert multifaceted impacts on both climate and human health across a range of environments (Wang and Penner, 2009; Rosenfeld et al., 2014; Shiraiwa et al., 2017; Bellouin et al., 2020; Carslaw, 2022; Rosenfeld et al., 2008). Atmospheric new particle formation (NPF), a significant contributor to aerosol number concentration, involves the formation of stable molecular clusters and their subsequent growth through the condensation of precursor vapours (Merikanto et al., 2009; Spracklen et al., 2010; Kerminen et al., 2018; Kulmala, 2003). While both the nucleation and growth of new particles are commonly linked to sulfuric acid (H_2SO_4) owing to its low volatility, H_2SO_4 and its inorganic clusters (e.g. H_2SO_4-NH_3 clusters) alone are insufficient to explain the rapid nucleation rates observed in forested regions minimally affected by anthropogenic pollution (Kuang et al., 2008; Sihto et al., 2006; Kerminen et al., 2018; Stolzenburg et al., 2020; Weber et al., 1997; Boy et al., 2008; Paasonen et al., 2010; Andreae et al., 2022). Furthermore, while H_2SO_4 frequently initiates cluster formation, its concentration does not account for the high growth rates of particles larger than 3 nm diameter (Ehn et al., 2014; Deng et al., 2020).

Laboratory studies and ambient measurements have shown that highly oxygenated organic molecules (HOMs) largely account for the particle nucleation and growth rate in forested areas owing to their extremely low volatility. Riccobono et al. (2014) revealed a nucleation mechanism involving both H_2SO_4 and oxidized organic molecules from the very first step, and including this mechanism in a global aerosol model yielded a seasonal cycle of particle concentrations in the continental boundary layer, in good agreement with observations. Jokinen et al. (2015) found monoterpene-derived HOMs promote NPF under continental conditions using chamber experiments. Kirkby et al. (2016) showed that the rate of formation of particles from biogenic HOMs, in the absence of H_2SO_4, can be enhanced by 1–2 orders of magnitude by ions based on CERN CLOUD (Organisation Européene pour la Recherche Nucléaire - Cosmics Leaving Outdoor Droplets) experiments. In addition to contributing to the formation of 1-2 nm clusters, Ehn et al. (2014) showed HOMs made important contributions to the particle growth with diameters between 5 and 50 nm in northern forests, which was recently explained by Mohr et al. (2019) at the molecular level. Bianchi et al. (2016) also showed observational evidence that NPF occurs mainly through condensation of HOMs at high altitude.

Although HOMs are necessary for NPF in the absence of H_2SO_4 (Kirkby et al., 2016), the molecular structures and formation pathways of HOMs remain uncertain and are treated in a variety of ways in models. Gordon et al. (2016) simulated monoter-

https://doi.org/10.5194/egusphere-2024-401
Preprint. Discussion started: 13 February 2024

pene-derived HOMs formation using an empirical or semiempirical fixed yield of HOMs from first stage monoterpene oxidation products, although with a highly simplified HOMs chemistry. Zhu et al. (2019) added some explicit chemical mechanisms for HOMs, but they did not consider autoxidation and used a less stringent definition of HOMs than recommended in Bianchi et al. (2019). Roldin et al. (2019) used a more explicit reaction mechanism to treat the generation of HOMs through autoxidation and cross-reactions of α-pinene oxidation products in a 1-D column model. Weber et al. (2020) used a similarly explicit mechanism over the boreal forest in Finland and the southeast USA, although not on a global scale.

There is thus a lack of global-scale simulations of NPF with explicit HOMs chemistry and quantification of the contribution of organics to aerosol and CCN number concentrations. Recently, Xu et al. (2022) summarized the various chemical mechanisms of HOMs, including monoterpene-derived peroxy radical (MT-RO_2) unimolecular autoxidation and self- and cross-reactions with other RO_2 species, and evaluated them in the GEOS-Chem global model. However, they did not quantify the effects of HOMs participating in NPF. Here, we incorporate the representation of HOMs from Xu et al. (2022) within a global chemistry-climate model and then quantify the contribution of HOMs to aerosol number concentration globally. Inorganic nucleation rates involving H_2SO_4 and NH_3 as well as ion-induced pathways based on the CLOUD chamber experiments are also included (Dunne et al., 2016), replacing a simpler scheme based on H_2SO_4 and NH_3 (Vehkamaki et al., 2002; Merikanto et al., 2007).

The model and field measurements used in this study are documented in Section 2. Section 3 evaluates outputs of the updated model, including nucleation and growth rates, frequencies of NPF events, and aerosol number concentrations. Additionally, four sensitivity experiments aimed at investigating uncertainties in concentrations of organic nucleating species and disentangling the roles of nucleation and growth processes are conducted. Section 4 quantifies the contributions of organic-related processes to nucleation rate, growth rate, aerosol and CCN number concentrations globally. Section 5 compares the proportion of organic nucleation rate with previous studies. Results are summarized and discussed in Section 6.

2 Data and methods

2.1 Model configuration

We use the atmospheric component of the Community Earth System Model (CESM) version 2.1.0, the Community Atmosphere Model version 6, augmented with comprehensive tropospheric and stratospheric chemistry (CAM6-Chem) (Emmons et al., 2020). Biogenic emissions are dynamically simulated using the Model of Emissions of Gases and Aerosol from Nature version 2.1 (MEGAN2.1) (Guenther et al., 2012). Anthropogenic and biomass burning emissions derive from the standard Coupled Model Intercomparison Project round 6 (CMIP6) (Eyring et al., 2016), with emissions in China replaced by the multi-resolution emission inventory for China (MEIC, http://www.meicmodel.org) (Li et al., 2017; Yue et al., 2023) which considerably improves Chinese emission inventories compared to the earlier large-scale studies (Zheng et al., 2009; Zhou et al.,

https://doi.org/10.5194/egusphere-2024-401
Preprint. Discussion started: 13 February 2024

2017). CAM6-Chem utilizes a four-mode version of the Modal Aerosol Module (MAM4) (Liu et al., 2016), coupled with the Model for Simulating Aerosol Interactions and Chemistry (MOSAIC) (Zaveri et al., 2021) to explicitly represent the heterogeneous uptake of isoprene-epoxydiols (IEPOX) onto sulfate aerosols and subsequent production of isoprene-epoxydiols (Jo et al., 2019; 2021). Following Liu et al. (2023), we adopt a modest photolysis rate for monoterpene-derived secondary organic aerosols, constituting 2.0% of the NO_2 photolysis frequency (Bianchi et al., 2019; Krapf et al., 2016; Zawadowicz et al., 2020). All simulations were run at a horizontal resolution of 0.95° latitude and 1.25° longitude, with a vertical resolution extending up to approximately 40 km across 32 layers (Emmons et al., 2020). To follow the observed meteorological conditions and initialize realistic meteorological conditions, meteorological fields (temperature and wind profiles, surface pressure, surface stress, surface heat and moisture fluxes) are nudged toward Modern-Era Retrospective analysis for Research and Applications (MERRA2) reanalysis (Kooperman et al., 2012), which allows model-observation comparisons that are unaffected by variability in synoptic-scale model dynamics. We evaluate model performance against observations from multiple years (Section 3), where in each case the anthropogenic emissions and model meteorology correspond to values associated with the observation year.

We incorporate advanced chemical reactions involving the formation of HOMs, since in the default configuration of CAM6-Chem, organics are not involved in either the nucleation or the initial growth processes of aerosols (sub-20nm). These include MT-RO_2 unimolecular H shifts (i.e., "autoxidation") and self- and cross-reactions with other RO_2 species, guided by laboratory-derived mechanistic parameters from Xu et al. (2022). In total, 24 reactions in CAM6-Chem were modified and 96 reactions were added. Detailed descriptions of chemical mechanisms are shown in Liu et al. (2024), and the final products, including HOMs and accretion products (ACC, C15 and C20), are summarized in Table 1.

Table 1. The molecular formula, saturated vapor concentration (C*), enthalpy of vaporization (ΔH_{vap}) and corresponding volatility class of newly-added organics.

Species	Short Name	Molecular formula	log(C*) ($\mu g\ m^{-3}$)	ΔH_{vap} ($kJ\ mol^{-1}$)	Volatility Bin[a]
HOMs	C10-NON[b]	$C_{10}H_{14}O_9$	-3.22	164.0	LVOC
	C10-ON[c]	$C_{10}H_{14}O_9N$	-3.31	164.0	LVOC
ACC[d]	C15	$C_{15}H_{18}O_9$	-5.20	186.0	ELVOC
	C20	$C_{20}H_{32}O_8$	-9.53	230.0	ULVOC

[a] LVOC, ELVOC and ULVOC represent low/ extreme-low/ ultra-low volatility organic compounds, respectively.
[b] NON represents non-organonitrates.
[c] ON represents organonitrates.

https://doi.org/10.5194/egusphere-2024-401
Preprint. Discussion started: 13 February 2024

[d] ACC represents accretion products.

2.2 Nucleation and growth scheme in CAM6-Chem

2.2.1 Nucleation scheme in default CAM6-Chem

The default configuration of CAM6-Chem (Default, Table 2) includes binary homogeneous nucleation of H_2SO_4-H_2O (Vehkamaki et al., 2002) and ternary homogeneous nucleation of H_2SO_4-NH_3-H_2O (Merikanto et al., 2007). Additionally, within the boundary layer the model includes the empirical mechanism of Kulmala et al. (2006) and Sihto et al. (2006) as first used in a global model by Spracklen et al. (2006):

$$j_{1nm} = A\,[\mathrm{H_2SO_4}] \quad (1)$$

where A (1.0^{-6} s^{-1}) is the rate constant chosen from the median values derived in case studies (Sihto et al., 2006).

2.2.1 Updated inorganic nucleation scheme

Most existing models tend to overestimate the sensitivity of the nucleation rate to sulfuric acid concentrations when relying solely on classical nucleation theories of sulfuric acid (Ehn et al., 2014; Mann et al., 2014; Scott et al., 2014). Therefore our study updates the inorganic nucleation parameterizations in CAM6-Chem, drawing upon data from the CLOUD chamber experiments (Dunne et al., 2016). The updated schemes incorporate H_2SO_4, NH_3 and ions. The inorganic NPF rates at a mobility equivalent diameter of 1.7 nm are calculated by summing the following rates (Dunne et al., 2016):

1. Binary neutral (indicated by b,n, J_{SA}) and ion-induced (b,i, $J_{SA,i}$) NPF involving sulfuric acid and water:

$$J_{\mathrm{SA}} = K_{b,n}(T)[\mathrm{H_2SO_4}]^{P_{b,n}} \quad (2)$$

$$J_{\mathrm{SA,i}} = K_{b,i}(T)[\mathrm{H_2SO_4}]^{P_{b,i}}\,[n-] \quad (3)$$

$K(T)$ are temperature-dependent prefactors, P_i are constant parameters, and $[n-]$ is the concentration of negative ions produced from galactic cosmic rays (equal to $[n\pm]$ in Eq. (8), which is parameterized in the Text S1).

2. Ternary neutral (indicated by t,n, $J_{SA\text{-}NH3}$) and ion-induced (t,i, $J_{SA\text{-}NH3,i}$) NPF involving sulfuric acid, ammonia and water:

$$J_{\mathrm{SA-NH3}} = K_{t,n}(T)f_n([\mathrm{NH_3}],[\mathrm{H_2SO_4}])[\mathrm{H_2SO_4}]^{P_{t,n}} \quad (4)$$

$$J_{\mathrm{SA-NH3,i}} = K_{t,i}(T)f_i([\mathrm{NH_3}],[\mathrm{H_2SO_4}])[\mathrm{H_2SO_4}]^{P_{t,i}}\,[n-] \quad (5)$$

where the f ([NH_3], [H_2SO_4]) are functions of the ammonia and sulfuric acid gas phase concentrations, also involving free-fitting parameters.

https://doi.org/10.5194/egusphere-2024-401
Preprint. Discussion started: 13 February 2024

2.2.2 New organic nucleation scheme

There is no organic nucleation scheme in the Default (Table 2) so organic NPF rates at 1.7 nm mobility equivalent diameter were included as the sum of the following parameterizations:

1. The rate of heteromolecular nucleation of sulfuric acid and organics (HET, $J_{SA\text{-}Org}$) is parameterized following Riccobono et al. (2014) depending on both H_2SO_4 and organic nucleating species concentration:

$$J_{SA-Org} = K_m\ [H_2SO_4]^2\ [HOM + ACC] \quad (6)$$

where ACC are accretion products (Table 1) and K_m is the multicomponent prefactor, which equals to 3.27×10^{-21} cm^6 s^{-1} (Riccobono et al., 2014).

2. The rate of neutral pure organic nucleation (NON, $J_{Org,n}$) and ion-induced pure organic nucleation (ION, $J_{Org,i}$) are parameterized based on Kirkby et al. (2016):

$$J_{Org,n} = a_1\ [ACC]^{\,a_2+\frac{a_5}{[ACC]}} \quad (7)$$

$$J_{Org,i} = [n\pm]a_3\ [ACC]^{\,a_4+\frac{a_5}{[ACC]}} \quad (8)$$

where ACC are in units of 10^7 molecules cm^{-3}, parameters a_n are determined from fits to experimental data (Dunne et al., 2016), and $[n\pm]$ is the ion concentration produced from galactic cosmic rays (Text S1). A temperature dependence for the organic nucleation rates was introduced by multiplying by exp (-(T-278)/10) as suggested in Dunne et al. (2016).

2.2.3 Updated particle growth scheme

The growth rate of nuclei is important for the survival probability up to larger sizes and eventually contribution to CCN (Pierce and Adams, 2009; McMurry et al., 2005). The effective production rate of 20 nm diameter particles (the smallest size simulated by the model) is calculated from the Kerminen and Kulmala (2002) formula:

$$j_{20nm} = j_{1.7\ nm} \exp\left[-0.66\frac{\gamma CS}{GR}\right] \quad (9)$$

where CS is the reduced (simplified) condensation sink, γ is a proportionality factor and GR is the growth rate.

In the Default simulation, sub-20nm particle growth is solely caused by condensation of H_2SO_4 and is approximated as Kerminen and Kulmala (2002):

$$GR = \frac{3.0\ \times 10^{-9}}{\rho}\ v_{H2SO4}\ M_{H2SO4}\ c_{H2SO4} \quad (10)$$

where v_{H2SO4} is the mean molecular speed of H_2SO_4, M_{H2SO4} is the molecular weight of H_2SO_4, c_{H2SO4} is the gas phase concentration of H_2SO_4, and ρ is the density of the nuclei. 3.0×10^{-9} is approximation of the product of many parameters (Kerminen and Kulmala, 2002).

https://doi.org/10.5194/egusphere-2024-401
Preprint. Discussion started: 13 February 2024

Neglecting organic vapor condensation on sub-20nm particles will lead to insufficient growth rates and potentially reduced survival of newly formed particles (Pierce and Adams, 2009). Therefore, the condensation of monoterpene-derived condensable organic compounds (COC) (including HOMs and ACC) to newly formed particles is added in our updated model. The enhanced growth rate of particles from 1 nm to 20 nm is then parameterized as follows:

$$GR = \frac{3.0 \times 10^{-9}}{\rho} \left(v_{H2SO4} \times M_{H2SO4} \times c_{H2SO4} + v_{COC} \times M_{COC} \times [c_{COC} - c^*_{COC}]\right) \quad (11)$$

where v_{COC} is the mean molecular speed of COC (ACC and HOMs), M_{COC} is the molecular weight of COC, c_{COC} is the gas phase concentration of COC, and c^*_{COC} is saturated vapor concentration of COC which is parameterized in Text S2.

Simulations with the updated inorganic nucleation scheme (i.e. Eq. (2)-(5)) are named "Inorg" and simulations including also the new organic mechanisms (i.e. Eq. (6)-(8) and (11)) are named "Inorg_Org" (Table 2).

2.3 Method of evaluating NPF-related variables

In addition to evaluating aerosol concentrations, we also evaluate NPF event properties in terms of the nucleation rate, growth rate and frequency of occurrence of NPF events. CAM6-Chem does not incorporate a nucleation mode, so we employ a threshold of j_{20nm} (Eq. (9)) to define the occurrence of NPF events (i.e., when j_{20nm} > threshold). Then we could evaluate the NPF frequency (fraction of days) by defining an "NPF day" as a day during which j_{20nm} is higher than a threshold value. Also, the method to evaluate these NPF properties during "NPF day" is described in Text S3.

2.4 Sensitivity experiments

We performed two simulations to quantify the relative contribution of the nucleation rate (Only_NR) and growth rate (Only_GR) to aerosol concentrations in order to separate the contribution of the organic compounds to each of these processes. The Only_NR and Only_GR simulations employ the same settings as Inorg_Org (Table 2), but in Only_NR the organic-involved particle growth is disabled (i.e., Eq. (10) is used instead) and in Only_GR the organic-involved nucleation rates (i.e., Eq. (6)-(8)) are disabled.

We also conducted two sensitivity simulations to examine uncertainties in concentrations of HOMs (Table 2): sensitivity to the branching ratio from the first generation of monoterpene (MT) reactions with O_3/OH that can be auto-oxidized (Low_Br) and sensitivity to the rate of termination reaction involving NO (Slow_NO) (Table 2). In Inorg_Org, the branching ratios for the MT-derived peroxyl radicals (MT-RO_2) which could be further auto-oxidized are set at 80% for MT+O_3 and 97% for MT+OH reactions, corresponding to the high values reported in Xu et al. (2022). In the Low_Br simulation (Table 2), the branching ratio for MT-RO_2 is set as 25% for MT + O_3 and 92% and MT + OH. Both the high and low branching ratios fall within the range of previous studies (Lee et al., 2023; Pye et al., 2019; Weber et al., 2020; Xu et al., 2018; Jokinen et al., 2015;

https://doi.org/10.5194/egusphere-2024-401
Preprint. Discussion started: 13 February 2024

Roldin et al., 2019). In Slow_NO, the reaction rate of MT-HOM-RO_2+NO (MT-HOM-RO_2, the second-generation product of auto-oxidation (Liu et al. (2024)) is set as one-fifth of that in Inorg_Org, given that the simulated NO concentration is fourfold higher than the measured values in the boreal forest in Finland and in the southeast USA (Fig. S2 and S2 in Liu et al. (2024)).

Table 2. Configurations of CESM2.1.0 Experiments

Test Name	Updated inorganic nucleation	HOMs chemistry	Organic Nucleation	Organic Growth	Other Changes
Default	×	×	×	×	/
Inorg	✓	✓	×	×	/
Inorg_Org	✓	✓	✓	✓	/
Only_NR	✓	✓	✓	×	/
Only_GR	✓	✓	×	✓	/
Low_Br	✓	✓	✓	✓	Lower branch ratio of the first generation product (MT-RO_2) from MT + O_3 and MT + OH, which could be further auto-oxidized
Slow_NO	✓	✓	✓	✓	Rate of MT-HOM-RO_2 + NO generating HOMs, multiplied by 0.2

2.5 Observation data

Observational data used in this study are from ships, stations, and aircraft (see Table 3). Measurements from the Canadian Aerosol Baseline Measurement Program (CABM), the Reactive Halogens in the Marine Boundary Layer (RHaMBLe), and Aerosol-Cloud Coupling and Climate Interactions in the Arctic (ACCACIA) are compared with simulated N10 or N20 (number concentrations for particles with diameters larger than 10 nm or 20 nm), since these two variables are most sensitive to aerosol nucleation and initial growth. European Aerosol Cloud Climate and Air Quality Interactions projects (EUSAAR-EUCAARI) (Asmi et al., 2011; Kulmala et al., 2009) provides measured N30 and N50 (number concentrations for particles with diameters larger than 30 nm and 50 nm respectively) and these larger particles are more important for the condensation sink (CS) of HOMs and other precursor vapors during NPF. All above mentioned data were processed in the Global Aerosol Synthesis and Science Project (GASSP) (Reddington et al., 2017). Measured N20 and CCN concentrations at 0.5% supersaturation from the aircraft campaign Aerosol, Cloud, Precipitation, and Radiation Interactions and Dynamics of Convective Cloud Systems (ACRIDICON–CHUVA) (Wendisch et al., 2016) are used to examine the effect of the inclusion of organic NPF on the profile of CCN concentrations in an organic-dominated tropical environment. We also use ground station measurements of nucleation rates, growth rates, CS and NPF frequencies during specific time periods that correspond to the simulations. Full information of stations is listed in Tables S1 and S2.

https://doi.org/10.5194/egusphere-2024-401
Preprint. Discussion started: 13 February 2024

Table 3. Field measurements used in this study

Campaign	Platform	Dates	Region	Variables
RHaMBLe (http://www.cas.manchester.ac.uk/re-sprojects/rhamble/cruise/)	Ship	17 May – 9 June 2007	North Atlantic Ocean (-25.05° W – 8.35° W; 16.32 – 46.14° N)	N10
ACCACIA (http://arcticaccacia.wordpress.com)	Ship	12 July – 13 August 2013	Arctic between Norway and Svalbard (20.70 – 34.84° E; 55.73 – 83.32° N)	N10
CABM (https://ec.gc.ca/air-sc-r)	Station	23 October 2012 – 1 January 2013	Ellesmere Island, Canada (62.34° W, 82.49° N) Egbert, Canada (79.78° W, 44.23° N)	N20
EUSAAR-EUCAARI (Asmi et al., 2011)	Station	1 January 2008 – 1 January 2010	Europe	N30, N50
ACRIDICON–CHUVA (Andreae et al., 2018)	Aircraft	September 2014	Amazon Basin	N20 CCN (0.5%ss)

3 Evaluation of the updated NPF scheme

In this section, we evaluate the results derived from the updated model (Inorg_Org) and focus on the comparison between Inorg_Org and Inorg (definitions in Table 2). Specifically, we compare nucleation rate, sub-20nm particle growth rate, NPF event frequency, and condensation sink (CS) (Fig. 1) between simulations and measurements. Results from sensitivity tests (Low_Br and Slow_NO) are used to evaluate the effect of uncertainties in HOMs chemistry on aerosol (Fig. 2 and 3) and CCN concentrations (Fig. 4).

3.1 Evaluation of NPF-related variables

The properties of the nucleation events themselves (formation rates, growth rates, and event frequencies) provide the best test of NPF schemes, while state variables like particle concentration have many other sources of error in a model.

As shown in Fig. 1a, at most grounds stations, the nucleation rate in Inorg_Org agrees better with measurements than Inorg (normalized mean bias, NMB changes from -97% in Inorg to -64% in Inorg_Org). The improvement is particularly clear in non-urban areas where biogenic organic nucleation plays a substantial role, such as Hyytiälä, Ozark Forest, Po Valley and Leicester (NMB changes from -92% in Inorg to -34% in Inorg_Org, Fig. 1a). In these regions, the nucleation rate increases by at least a factor of 8 when the organic nucleation mechanisms are included (Inorg_Org compared to Inorg). In Toronto and

https://doi.org/10.5194/egusphere-2024-401
Preprint. Discussion started: 13 February 2024

Gadanki, the nucleation rate becomes detectable following the incorporation of organic nucleation mechanisms, in good agreement with observations (9.2 cm^{-3} s^{-1} in Inorg_Org compared to 12.9 cm^{-3} s^{-1} measurement of Toronto; 1.6cm^{-3} s^{-1} in Inorg_Org compared to 1.2 cm^{-3} s^{-1} in measurement of Gadanki, Table S1). However, in multiple urban regions of China, the nucleation rate remains underestimated (NMB>-50%). This is likely because the effects of anthropogenic-derived HOMs and amines are not accounted for in this study, and these effects will be strongest in urban regions. Hong Kong serves as a stark example, where the nucleation rate shows minimal change when the biogenic-organic nucleation scheme is implemented, rising slightly from 0.3 cm^{-3} s^{-1} (Inorg) to 0.31 cm^{-3} s^{-1} (Inorg_Org). Several other Chinese megacities, including Beijing and Nanjing, show similar behaviour.

Figure 1b shows that the growth rate in Inorg is underestimated (NMB = -54%) but is overestimated at most sites in Inorg_Org (NMB = 39%). One contributing factor is the overestimation of H_2SO_4 concentration, a feature of CAM6, as evidenced by comparisons with previous model simulations (Table S3) and measurements (Table S4). This discrepancy is particularly noticeable in China, where H_2SO_4 dominates the growth rate (will be further discussed in Fig. 7, Section 4). This is also supported by overestimated growth rates in Beijing, Qingdao, and Hongkong in Inorg, which considers only H_2SO_4 contribution to sub-20nm growth. This suggests excessive H_2SO_4 is a feature of the default model. The growth rate of new particles in Hong Kong is zero (Fig. 1b) since there are almost no newly formed particles (nucleation rate ~ 0 cm^{-3} s^{-1}, Fig. 1a).

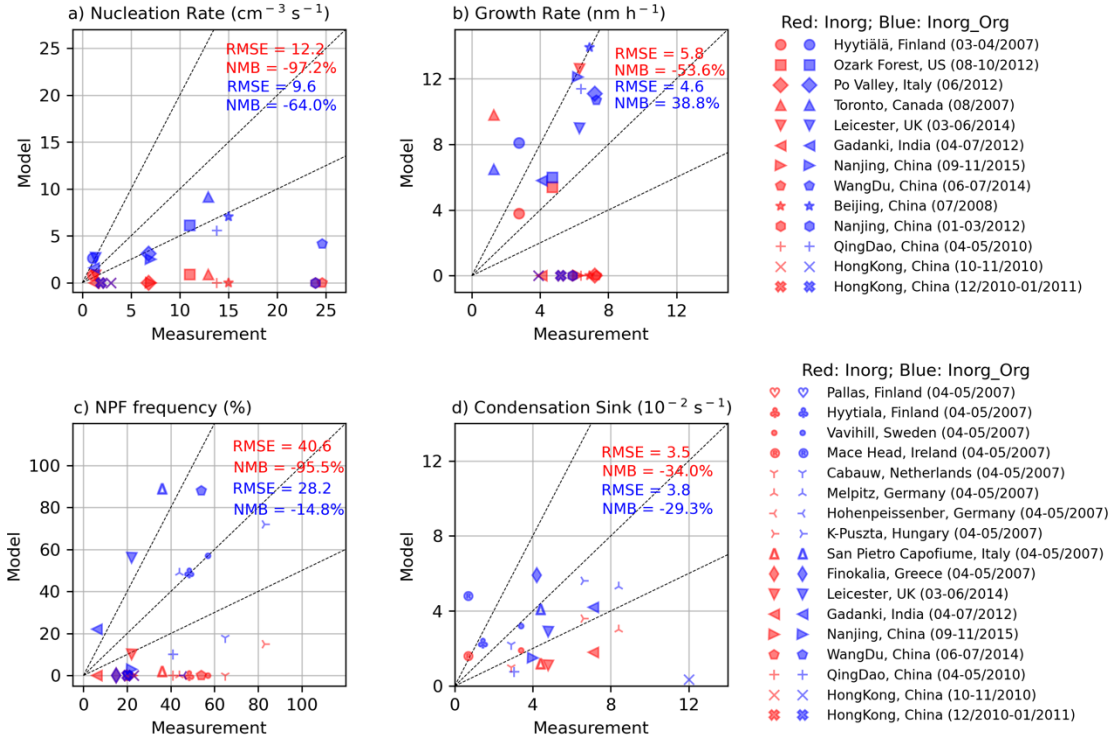

https://doi.org/10.5194/egusphere-2024-401
Preprint. Discussion started: 13 February 2024

Figure 1: Comparison of simulated (choosing median value of measured smallest nucleation rates as threshold, see Text S3) and measured (a) nucleation rate, (b) growth rate, (c) NPF frequency, and (d) condensation sink in Inorg_Org (blue symbols) and Inorg (red symbols). Information regarding the measurement sites is summarized in Tables S1. Root mean square error (RMSE) and normalized mean bias (NMB) values are shown. (a) and (b) use the same dataset. (c) and (d) use the same dataset.

NPF events are far more frequent in Inorg_Org than in Inorg (NMB in NPF frequency changes from -96% to -15%) (Fig. 1c). Simulated NPF frequencies in Inorg_Org agree better with measurements in Europe (Hyytiälä, Vavihill, Cabauw, Melpitz and K-Puszta) – see Table S2. Inorg_Org tends to overestimate NPF frequencies (by a factor 2) in some rural and forested areas such as the San Pietro Capofiume, Leicester, and Wangdu and significantly underestimates frequencies in Chinese urban areas like Nanjing and Hong Kong (more than 3 times, Fig. 1a). These discrepancies are consistent with the nucleation rates discussed earlier (Table S1). In some locations (Melpitz, San Pietro Capofiume, Leicaster and Gadanki) the overestimation of NPF frequency in Inorg_Org is consistent with an underestimation of CS and, vice versa, the underestimation of NPF frequency in Finokalia is consistent with an overestimation of CS (Figs. 1c and 1d).

3.2 Evaluation of aerosol and CCN number concentrations

To better understand the influence of implementing the new nucleation schemes, model-simulated particle number concentrations are evaluated against shipborne measurements over the ocean and CCN concentrations are evaluated using measurements from Amazonia. We also discuss the influence of uncertainties in HOMs chemistry. Unlike in Spracklen et al. (2010), the lack of a nucleation mode in CAM means that we cannot use extensive measurements from condensation particle counters.

The values of number concentrations for particles with diameters larger than 10 nm (N10) in Inorg_Org agree better with measurements over ocean (Figs. 2 and 3) but number concentrations for particles with diameters larger than 20 nm (N20) are overestimated in continental regions at surface level (Fig. 4). From Figs. 2 and 3, N10 in Inorg_Org are the closest to measurements in both the North Atlantic and the Arctic when considering both normalized mean bias (NMB) and root mean square error (RMSE). The Inorg_Org (Figs. 2e, f and 3e, f) alleviates both overestimation of N10 in Default resulting from their high sensitivity to H_2SO_4 concentrations (see Fig. 2a, b and 3a, b), and underestimation at some sites in Inorg caused by the lack of organics participating NPF (Fig. 2c, d and 3c, d). The influence of HOMs chemistry to N10 will be discussed in Section 3.3. In boreal Canada (Fig. 4), N20 are overestimated in Inorg_Org during the summer when NPF is particularly active. The overestimation is more significant at Egbert, located just 80 km north of Toronto, where Inorg shows better agreements with measurements. This discrepancy is likely due to an about 30% overestimation of growth rates (in Toronto, Table S1) and the underestimation of the N50 during Northern hemisphere summer (as relevant to CS) at many stations in Inorg_Org (N50 in Fig. S8). The underestimation of the N50 also explains the overestimation of N20 observed at the surface level in Amazonia in September 2014 (Fig. 4c) where insufficient large aerosols (N50, Fig. S8) result in a low CS, which in turn leads to an excessive number of aerosols merging into the Aitken mode (N30, Fig. S7).

https://doi.org/10.5194/egusphere-2024-401
Preprint. Discussion started: 13 February 2024

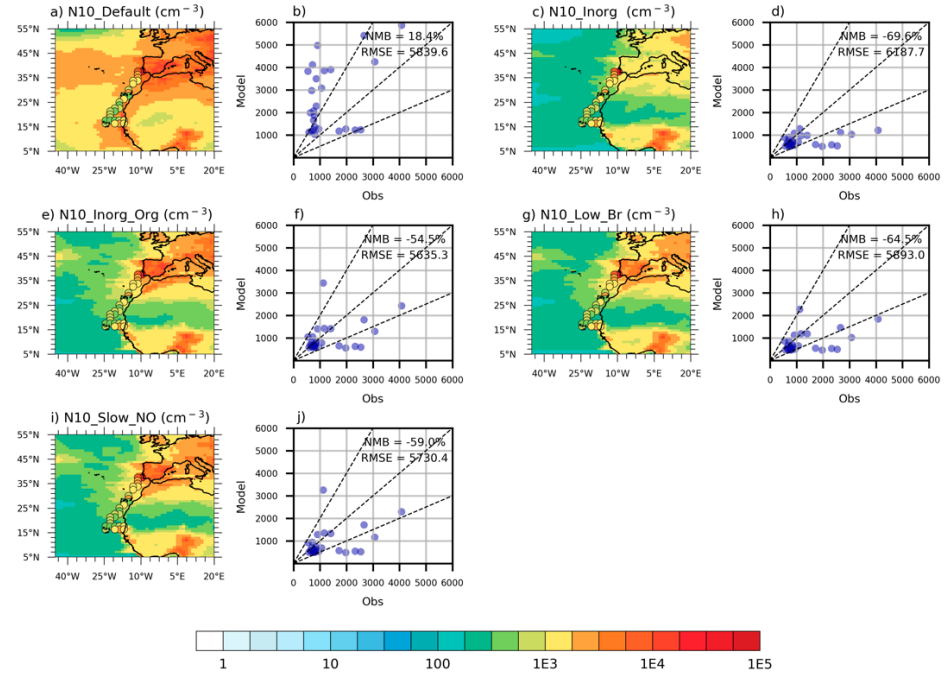

Figure 2: N10 concentration in the North Atlantic from (a, b) Default, (c, d) Inorg, (e, f) Inorg_Org, (g, h) Low_Br, and (i, j) Slow_NO (Unit: cm^{-3}). N10 from RHaMBLe measurements are represented by filled circles. Model experiments are described in Table 2 and model data come from mean value of May 2007 outputs. Numbers at the upper right (Fig. 2b, d, f, h and j) indicate normalized mean bias (NMB) and root mean square error (RMSE).

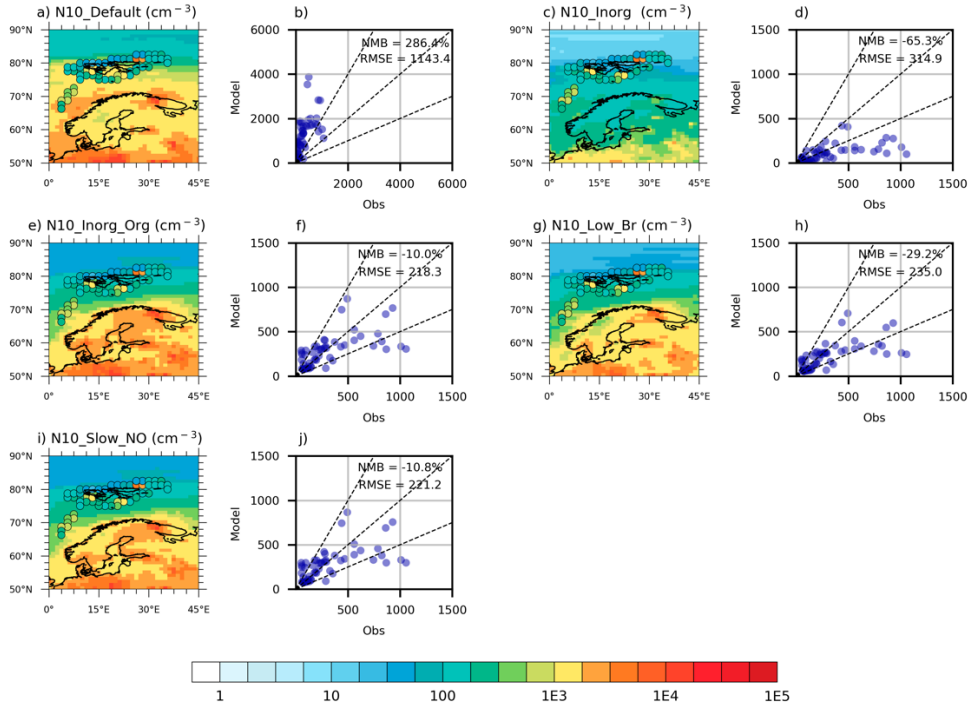

https://doi.org/10.5194/egusphere-2024-401
Preprint. Discussion started: 13 February 2024

Figure 3: N10 concentration in the Arctic from (a, b) Default, (c, d) Inorg, (e, f) Inorg_Org, (g, h) Low_Br and (i, j) Slow_NO (Unit: cm^{-3}). N10 from ACCACIA measurements are represented by filled circles. Model experiments are described in Table 2 and model data come from mean value of July 2013 outputs. Numbers at the upper right (Fig. 3b, d, f, h and j) indicate normalized mean bias (NMB) and root mean square error (RMSE).

After incorporating organic-related process, CCN at high altitude of Amazonia perform better compared with measurements. While all simulations considerably overestimate CCN concentrations at 0.5% supersaturation (0.5% ss) at surface level, CCN in the upper troposphere (5-12 km) in Inorg_Org (blue line, Fig. 4d) are the closest to measurements compared with both Default and Inorg. The more than 100% increase in CCN number at 8-12 km is mainly attributed to effective vertical transport of accretion products (ACC), which have longer atmospheric lifetime compared to HOMs (Xu et al., 2022) and then participate in $J_{Org,n}$ and $J_{Org,i}$ (Figs. 6c and 6e), thereby increasing N20 and CCN concentrations at high levels. N20 shows the highest value at about 6km altitude since nucleating speices are abundant there and the condendation sink is relatively low (see CCN profile in Fig. 4d) compared to higher altitude.

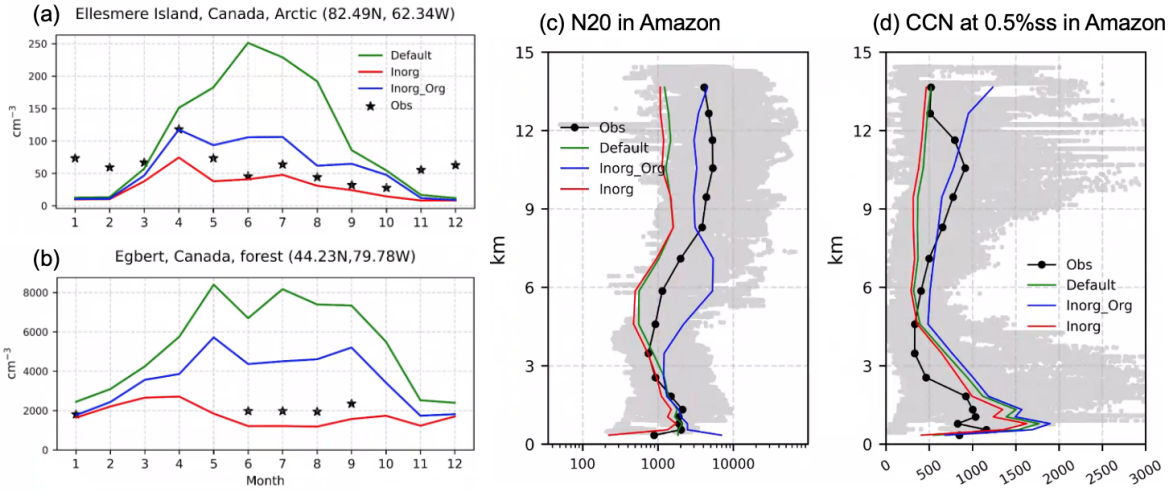

Figure 4: Seasonal variation in 2013 at two Canadian sites (a) Ellesmere Island, and (b) Egbert. Vertical profiles of (c) N20 and (d) CCN at a supersaturation of 0.5% in the Amazon basin, measured at standard temperature and pressure (STP) (unit: cm^{-3}), in September 2014.

3.3 Evaluation of uncertainty in HOMs chemistry

Uncertainties from HOMs chemistry (Low_Br and Slow_NO) do not affect N10, N20 and CCN number significantly. Compared to Inorg_Org, relative differences of RMSE from N10 over oceans in Low_Br (Figs. 2g, h and 3g, h) and Slow_NO (Figs. 2i, j and 3i, j) are within 10%. Similarly, in Low_Br and Slow_NO, CCN number do not show significant change over Amazonia compared to Inorg_Org (within 5%). This is because $J_{Org,i}$ and $J_{Org,n}$ contribute a lot in Amazonia but HOMs only participate in $J_{SA\text{-}Org}$ (Figs. 6d and 6f). Therefore, Inorg_Org can serve as a basis for further quantification of organic contributions in Section 4.

https://doi.org/10.5194/egusphere-2024-401
Preprint. Discussion started: 13 February 2024

4 Quantifying the effect of organics-NPF on global aerosol

In this section, we use simulation results to quantify how HOMs affect the nucleation rate (Figs. 5 and 6), growth rate (Fig. 7), particle number (Fig. 8), and CCN number (Fig. 10) on a global scale. Additionally, results from sensitivity tests (Table 2) are also analyzed to reveal the influence of uncertainty from chemical mechanisms of HOMs and the relative importance of organic nucleation and initial growth process to particle number (Fig. 9).

Globally, the vertically-integrated (below 15 km) annual mean organic nucleation rate in Inorg_Org is 32 $\times 10^6$ cm^{-2} s^{-1} (Fig. 5a), closely matching the inorganic nucleation rate of 39 $\times 10^6$ cm^{-2} s^{-1} (Table 4). $J_{SA\text{-}Org}$ contributes most to the total nucleation rate (45%), average value of 31.8$\times 10^6$ cm^{-2} s^{-1} (Table 4), and its spatial distribution (Fig. 6a) is influenced by both H_2SO_4 and HOMs concentrations. In regions abundant in HOMs (like boreal forest, North America and Australia in Fig. S4), the rate surges to 10^8 cm^{-2} s^{-1} (Fig. 5a) and the organic contribution exceeds 80% (Fig. 5c). High concentrations of ACC are simulated in Amazonia (Fig. S5), where ACC are transported to high altitudes through strong convection (Section 3), thereby resulting in high rates of $J_{Org,i}$ (over 40%, Fig. 6f). H_2SO_4-NH_3 neutral nucleation comprises the largest proportion of inorganic nucleation rate (>80% of inorganic and 40.5% of total nucleation rate, Table 4), particularly in China and India due to high anthropogenic SO_2 emission. This is also consistent with the spatial distribution of H_2SO_4 (Fig. S3). The contribution of H_2SO_4-NH_3 neutral nucleation makes up more than 50% of the nucleation rate over coastal regions where HOMs and accretion products (ACC) are less abundant (Fig. S4 and S5) and the large proportion in Africa is due to high NH_3 column concentration (Luo et al., 2022).

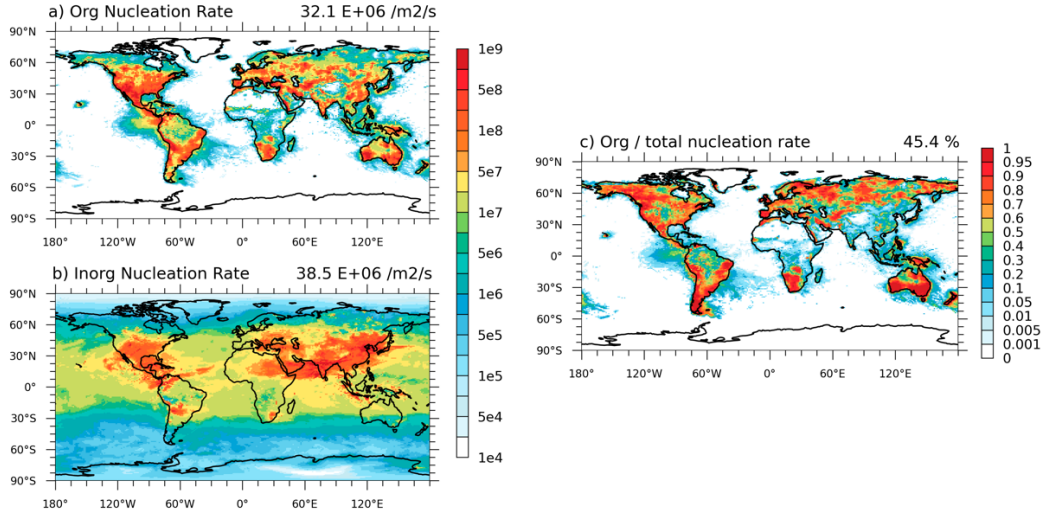

Figure 5: Spatial distribution of the 2013 annual mean nucleation rate (j_{1nm}, vertically-integrated below 15 km) attributed to (a) organics and (b) H_2SO_4. (unit: m^{-2} s^{-1}) (c) is the proportion of organic nucleation proportion. Global mean values are shown on the top right of each figure.

https://doi.org/10.5194/egusphere-2024-401
Preprint. Discussion started: 13 February 2024

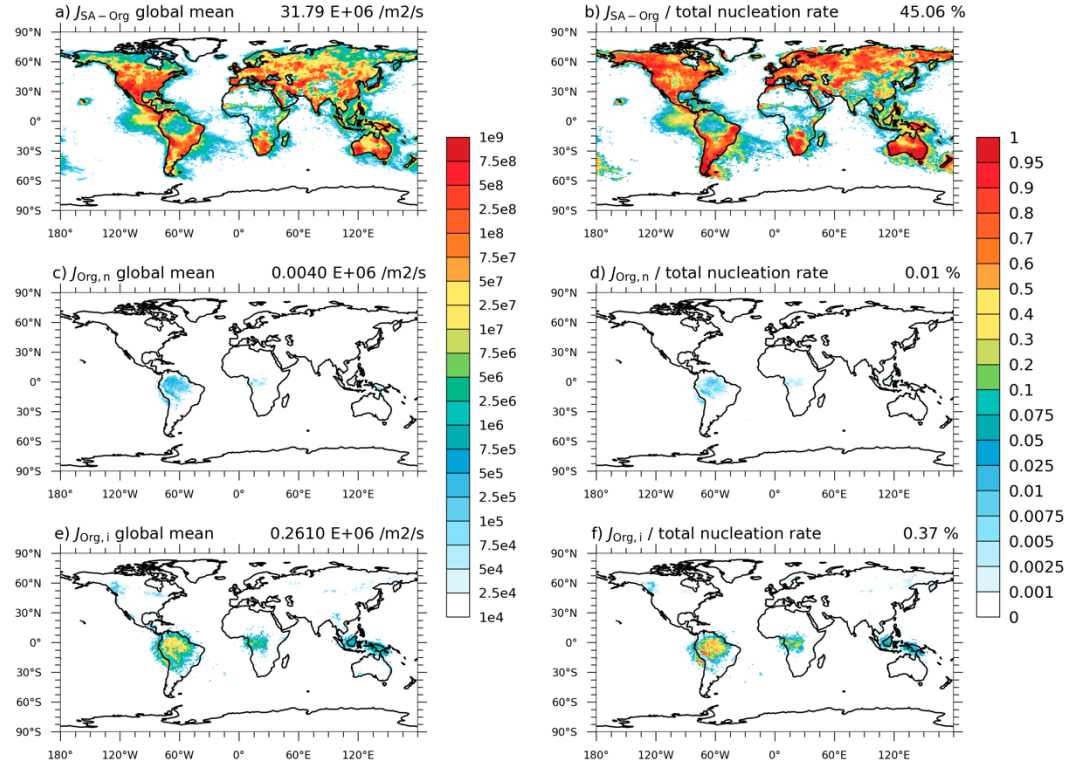

Figure 6: The 2013 annual average vertically-integrated organic nucleation rate (j_{1nm}) within the troposphere (a, c, e) (unit: m^{-2} s^{-1}) and their respective contributions (b, d, f) for J_{SA-Org} (a, b), $J_{Org,n}$ (c, d), and $J_{Org,i}$ (e, f) in the Inorg_Org. Global mean values are shown on the top right of each figure.

Table 4. The 2013 annual average vertically-integrated organic nucleation rate (j_{1nm}) within the troposphere and its contributions to total nucleation rates in the Inorg_Org.

Pathways	Nucleation Rate (Unit: 10^6 m^{-2}·s^{-1})	Proportion
J_{SA}	3.09	4.38%
$J_{SA,i}$	2.62	3.71%
J_{SA-NH3}	3.09	40.48%
$J_{SA-NH3,i}$	4.22	5.99%
$J_{Org,n}$	0.40	0.01%
$J_{Org,i}$	0.30	0.37%
J_{SA-Org}	31.80	45.06%

https://doi.org/10.5194/egusphere-2024-401
Preprint. Discussion started: 13 February 2024

Globally, the vertically-average (below 15 km) annual mean organic growth rate is 0.0048 nm h^{-1} (summation of ACC and HOMs contribution). The organic growth rate contributes to 25% of the total growth rate for sub-20nm particles. In regions such as Canada, the boreal forest, Amazonia, and Australia, where biogenic volatile organic compounds (BVOC) emissions dominate, organic growth accounts for over 60% of the total rate (Fig. 7c), consistent with the spatial distribution of HOMs and ACC (Fig. S4 and S5). Conversely, in China and India, H_2SO_4 exerts a predominant influence (> 90%) on the initial growth of new particles, with a rate of approximately 0.1 nm h^{-1}.

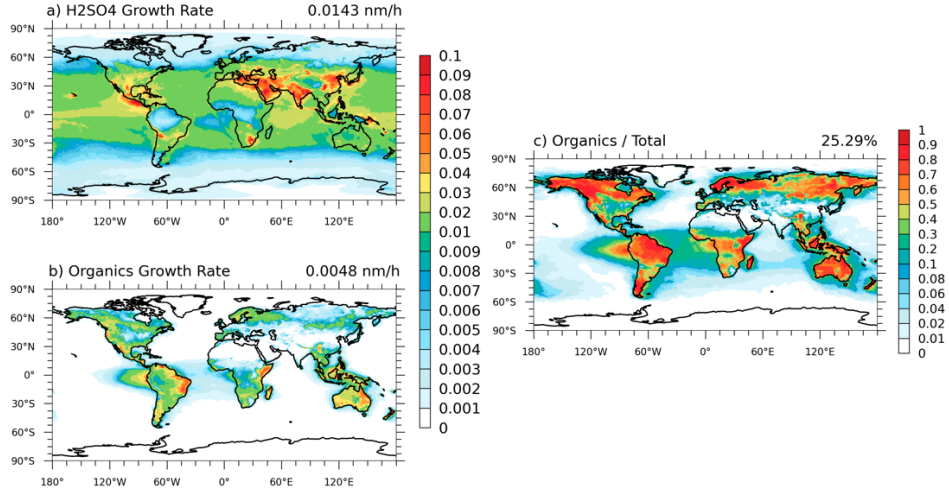

Figure 7: Spatial distribution of the 2013 annual mean vertically averaged growth rate attributed to (a) H_2SO_4, and (b) organics, along with the percentage of organics contributions (c). Global mean values are shown on the top right of each figure.

The global mean aerosol number burden increases by 39% (Fig. 8) in Inorg_Org compared to Inorg. The enhancement reaches a maximum of 60% in Amazonia due to high $J_{Org,i}$ (Fig. 6f) driven by high ACC concentrations (Fig. S5). Results from the Low_Br and Slow_NO simulations reveal that the uncertainties from HOMs chemistry have a negligible effect on the total aerosol number concentrations. Relative to Inorg_Org, Low_Br leads to an 12% reduction in number concentrations (Fig. 9f), although the branching ratio of MT-RO_2 shifts significantly (from 80 to 25% for the MT+O_3 reaction and from 97% to 92% for the MT+OH reaction). The impact of slowing down reaction rate of MT-HOM-RO_2 +NO (Slow_NO) is negligible globally (< 1%, Fig. 9h).

To evaluate the relative importance of organic contributions to nucleation and growth, we compare the Only_NR (no organic contribution to sub-20nm particle growth rate) and Only_GR (no organic contribution to 1nm particle nucleation rate) simulations. The global mean relative difference of aerosol number concentration between Only_GR (Fig. 9g) and Inorg_Org is 28% in a one-month simulation. Switching off growth alone (Only_NR) results in a 34% decrease in aerosol number relative to Inorg_Org (Fig. 9f). This illustrates that organic initial growth of new particles (sub-20nm) is slightly more important than organic nucleation for the production of particles larger than 20 nm diameter.

https://doi.org/10.5194/egusphere-2024-401
Preprint. Discussion started: 13 February 2024

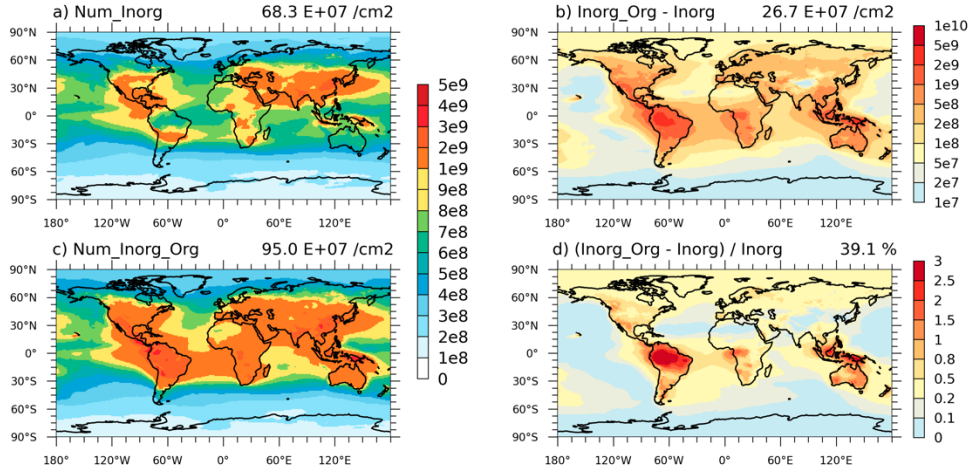

390 **Figure 8: Spatial distribution of annual mean total vertically-integrated particle number concentrations from (a) Inorg and (c) Inorg_Org (unit: cm^{-2}). Also, (b) change and (d) relative change are shown. Global mean values are shown on the top right of each figure.**

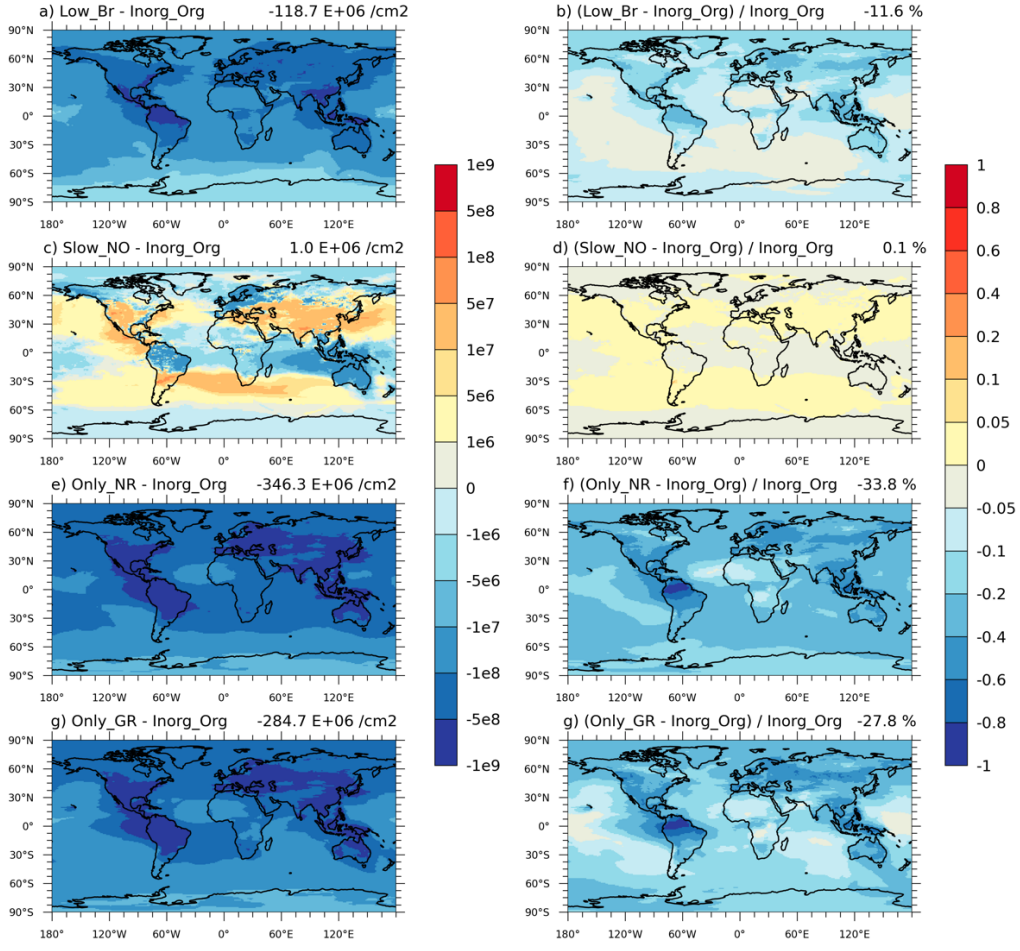

https://doi.org/10.5194/egusphere-2024-401
Preprint. Discussion started: 13 February 2024

Figure 9: Average changes (compared with Inorg_Org) in total vertically-integrated aerosol numbers in July 2013. (Units: cm^{-2}). Panels display (a) Only_NR – Inorg_Org, (c) Only_GR – Inorg_Org, (e) Low_Br – Inorg_Org, and (g) Slow_NO – Inorg_Org. Relative changes (compared with Inorg_Org) are shown for (b) Only_NR, (d) Only_GR, (f) Low_Br, and (h) Slow_NO. Global mean values are shown on the top right of each figure.

The global annual average CCN burden at 0.5% supersaturation increases by 33% upon adding organic NPF (Fig. 10). The spatial pattern of changes in CCN concentrations compared to Inorg is consistent with changes in aerosol number concentrations (Fig. 8), with increases predominantly occurring in regions abundant in HOMs and ACC (Fig. S4 and S5). Amazonia is the region most sensitive to organic-related processes due to high ACC concentrations (Fig. S5), where the total burden increases more than 100% (Fig. 10d).

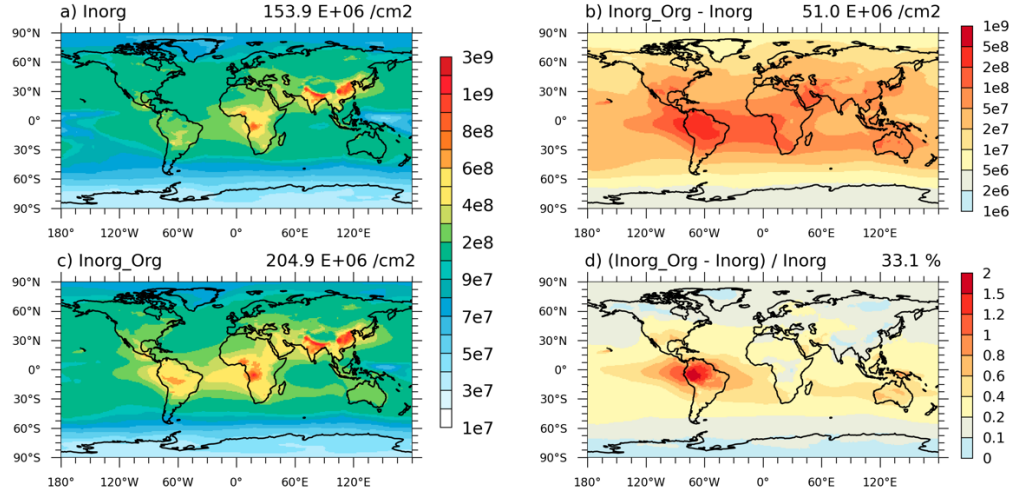

Figure 10: Spatial distribution of annual mean vertically-integrated CCN concentrations at 0.5% supersaturation for (a) Default, (d) Inorg, and (g) Inorg_Org (unit: cm^{-3}). The figure also presents percentage changes between each pair of scenarios (b, e, and h) and their relative differences (c, f, and i). Global mean values are shown on the top right of each figure.

5 Comparison with previous studies

Our results show that vertically-integrated organic nucleation contributes 84% of the total nucleation rate within the lower 5.8 km of the atmosphere, which is much higher than that in previous studies (51% in Gordon et al. (2017) and 42% in Zhu and Penner (2019), Table 5). The HOMs concentrations in our simulations are about 10 times greater than in Gordon et al. (2017), as depicted in Fig. S6 and Fig. S1 in Gordon et al. (2016). Here we used a chemical mechanism of HOMs derived from chamber experiments (including both auto-oxidation and self-/cross-reactions of isoprene/monoterpene-derived radicals) while Gordon et al. (2016) estimated HOMs concentrations using an empirical fixed yield from monoterpene+O_3/OH. Higher HOMs concentrations in our simulation are much closer to measurements in Finland and the southeast USA (Fig. S3 and S4 in Liu et al. (2024)), and lead to higher $J_{SA\text{-}Org}$.

https://doi.org/10.5194/egusphere-2024-401
Preprint. Discussion started: 13 February 2024

Updates to the inorganic nucleation scheme based on CLOUD chamber experiment data (Dunne et al., 2016) are the main reason we have higher contributions of vertically-integrated organic nucleation than Zhu and Penner (2019). The updated scheme decreases the inorganic nucleation rate by reducing its sensitivity to H_2SO_4 concentration. Thus, we simulate a higher organic nucleation proportion despite much lower $J_{Org,i}$ and $J_{Org,n}$. The lower values of $J_{Org,i}$ and $J_{Org,n}$ are caused by our use of a more stringent definition of organic participation (only ACC due to their extreme/ultra-low volatility) in neutral and ion-induced pure organic nucleation (NON and ION, Eq. (7) and (8)).

Table 5. Fractions of NPF from organic and inorganic pathways are derived from Inorg_Org (annual average in 2013 below 5.8 km altitude). Results from Gordon et al. (2017) and Zhu and Penner (2019) are in present-day experiments.

Pathways	Below 5.8 km vertical integration		
	Gordon et al. (2017)	Zhu and Penner (2019)	This study
J_{SA}	~0	58.40%	0.03 %
$J_{SA,i}$	7.50 %	w/o[a]	1.96 %
$J_{SA\text{-}NH3}$	17.00 %	w/o	6.18 %
$J_{SA\text{-}NH3,i}$	24.00 %	w/o	8.28 %
$J_{Org,n}$	~0	0.60%	~0
$J_{Org,i}$	4.10 %	23.20%	0.11 %
$J_{SA\text{-}Org,i}$[b]	14.00 %	w/o	w/o
$J_{SA\text{-}Org}$	33.00 %	17.80%	83.44 %

[a] w/o represents that there is no consideration of that nucleation scheme in publications
[b] $J_{SA\text{-}Org,i}$ represents that ion-induced heteromolecular nucleation of sulfuric acid and organics (HET).

Table 6. Annually averaged NPF from three organic pathways: vertically-integrated results across the whole atmosphere.

Pathways	Zhu and Penner (2019)[a]	This study [b]
$J_{SA\text{-}Org}$	34.4	33.0
$J_{Org,n}$	1.0	4.5 E-03
$J_{Org,i}$	52.9	0.3
Total	88.2	33.2

[a,b] Results are compared between present-day atmospheres (Zhu and Penner, 2019) and 2013 annual mean in this study.

https://doi.org/10.5194/egusphere-2024-401
Preprint. Discussion started: 13 February 2024

6 Summary and discussion

This study updates the inorganic nucleation scheme in CAM6-Chem according to chamber experimental measurements and adds organic nucleation and initial growth scheme based on a state-of-art chemical mechanism for biogenic highly oxygenated molecules (HOMs) including auto-oxidation and self-/cross-reactions of isoprene/monoterpene-derived radicals. The organic nucleation scheme includes heteromolecular nucleation of sulfuric acid and organics (HET), neutral pure organic nucleation (NON), and ion-induced pure organic nucleation (ION). Organic condensation on sub-20nm particles is also taken into account. The model was evaluated against new particle formation (NPF) events (occurrence frequency and nucleation and growth rates) as well as aerosol and cloud condensation nuclei (CCN) number concentrations. Finally, we quantified the contribution of organics to nucleation rate, growth rate, aerosol and CCN number at 0.5% supersaturation globally.

Compared to the model with updated inorganic nucleation mechanisms (Inorg), the revised model with HOMs chemistry (Inorg_Org) agrees better with measurements of the nucleation rate and sub-20nm particle growth rates at numerous sites globally (the normalized mean bias (NMB) of nucleation rate changes from -97% to -64% and the NMB of growth rate changes from -96% to -15%, Fig. 1). Inorg_Org also simulates NPF event frequency in better agreement with measurements at 17 sites compared to Inorg (NMB changes from -96% to -15%, Fig. 1), thereby accurately reproducing N10 (number concentrations for particles with diameters larger than 10 nm) ship-borne measurements over the Arctic and North Atlantic (Fig. 2 and 3). Both N20 (number concentrations for particles with diameters larger than 20 nm) and CCN concentration increase more than 100% between 8-12 km altitude (Fig. 4) over Amazonia after incorporating organic-related process and show better performance compared to aircraft measurements due to organic nucleating species (accretion productions) convection lifting to high level and then amplifying $J_{Org,i}$ (ION rate).

On a global scale, organics contribute 45% to the annual average vertically-integrated nucleation rate and 25% to the vertically averaged initial growth rate from Inorg_Org (global mean). Compared to Inorg, Inorg_Org increases the annual average vertically-integrated aerosol number concentration by 39%. The simulation shows that the organic-related growth process exerts a more substantial influence on aerosol number than nucleation. These newly-formed particles result in a 33% increase in annual average vertically-integrated CCN concentrations at 0.5% supersaturation compared to Inorg. Both aerosol and CCN concentrations display the most significant increase in Amazonia, exceeding 60% and 100%, respectively, attributable to its low aerosol concentration in Inorg in the background rainforest. More CCN produced through natural processes implies higher background aerosol abundance, thus weaker (less negative) historical aerosol forcing (Carslaw et al., 2013).

We also test the sensitivity of aerosol number concentrations to uncertainties from HOMs chemistry. Compared to Inorg_Org, decreasing the branch ratio of the first-generation product from Monoterpene+O_3/OH, which could further undergo auto-oxidation (Low_Br), leads to only a 12% reduction in global average vertically-integrated aerosol number concentrations. Slowing

https://doi.org/10.5194/egusphere-2024-401
Preprint. Discussion started: 13 February 2024

down NO-involved chemical reactions due to NO concentration overestimation at two stations (Slow_NO) does not change the global average aerosol number concentrations (within ~1%) (Fig. 10). These results suggest including the processes in our model is more important than tuning these aspects of the parametrisations.

The contribution of organic-involved nucleation to the vertically-integrated rate within the lower 5.8 km in our work (~83%) is significantly higher than previous studies. Compared to Gordon et al. (2017) (~51%), we use a more advanced HOMs chemistry that simulates higher HOMs concentrations in closer to measurements, thereby presenting higher $J_{SA\text{-}Org}$ (HET rate) and organics contribution. Compared to Zhu and Penner (2019) (~ 42%), we update the inorganic nucleation scheme based on CLOUD chamber experiments. Therefore, the inorganic nucleation rate and its proportion is reduced in our simulations and this provides a more reasonable baseline for the quantifying organic contribution. The greater contribution of biogenic organic nucleation to NPF implies that global aerosol may be more sensitive to changes in biogenic emissions. This finding should be tested with different representative concentration pathways (RCP) in the future, when human-induced global warming causes higher temperature and biogenic HOMs emissions, while emission reduction policies reduce anthropogenic emissions.

Given the limited knowledge of explicit chemical reactions forming anthropogenic-derived HOMs (Wang et al., 2017; Wang et al., 2020; Garmash et al., 2020; Molteni et al., 2018), we solely focus on organic nucleating species derived from monoterpene oxidation. This treatment likely leads to an underestimation of organic nucleation rates, particularly in urban areas (Fig. 1). More studies about chemical mechanisms of anthropogenic HOMs which could be applied globally are needed. Our work points out that subsequent growth of the newly formed particles to larger size may have a more significant effect on aerosol number than nucleation. More studies are needed to quantify the contribution of anthropogenic organics to initial growth rate. The change in simulated aerosol number and size distribution caused by anthropogenic HOMs-driven NPF can have important implications for CCN concentrations and aerosol indirect forcing, which also need further analysis (Wang and Penner, 2009; Wang et al., 2009; Gordon et al., 2016; Zhu et al., 2019).

Competing interests

At least one of the (co-)authors is a member of the editorial board of Atmospheric Chemistry and Physics.

Acknowledgments

This research is supported by the Natural Science Foundation of China (41925023, U2342223, 91744208,and 42075102). This research was also supported by the Collaborative Innovation Center of Climate Change, Jiangsu Province, and supported by the Frontiers Science Center for Critical Earth Material Cycling, Nanjing University. We greatly thank the High Performance Computing Center of Nanjing University for providing the computational resources used in this work. The CESM project is

https://doi.org/10.5194/egusphere-2024-401
Preprint. Discussion started: 13 February 2024

supported primarily by the United States National Science Foundation (NSF). This material is based upon work supported by the National Center for Atmospheric Research, which is a major facility sponsored by the NSF under Cooperative Agreement No. 1852977. We thank all the scientists, software engineers, and administrators who contributed to the development of CESM2.

References

Andreae, M. O., Andreae, T. W., Ditas, F., and Pöhlker, C.: Frequent new particle formation at remote sites in the subboreal forest of North America, Atmos. Chem. Phys., 22, 2487-2505, 10.5194/acp-22-2487-2022, 2022.

Andreae, M. O., Afchine, A., Albrecht, R., Holanda, B. A., Artaxo, P., Barbosa, H. M. J., Borrmann, S., Cecchini, M. A., Costa, A., Dollner, M., Fütterer, D., Järvinen, E., Jurkat, T., Klimach, T., Konemann, T., Knote, C., Krämer, M., Krisna, T., Machado, L. A. T., Mertes, S., Minikin, A., Pöhlker, C., Pöhlker, M. L., Pöschl, U., Rosenfeld, D., Sauer, D., Schlager, H., Schnaiter, M., Schneider, J., Schulz, C., Spanu, A., Sperling, V. B., Voigt, C., Walser, A., Wang, J., Weinzierl, B., Wendisch, M., and Ziereis, H.: Aerosol characteristics and particle production in the upper troposphere over the Amazon Basin, Atmos. Chem. Phys., 18, 921-961, 10.5194/acp-18-921-2018, 2018.

Asmi, A., Wiedensohler, A., Laj, P., Fjaeraa, A. M., Sellegri, K., Birmili, W., Weingartner, E., Baltensperger, U., Zdimal, V., Zikova, N., Putaud, J. P., Marinoni, A., Tunved, P., Hansson, H. C., Fiebig, M., Kivekäs, N., Lihavainen, H., Asmi, E., Ulevicius, V., Aalto, P. P., Swietlicki, E., Kristensson, A., Mihalopoulos, N., Kalivitis, N., Kalapov, I., Kiss, G., de Leeuw, G., Henzing, B., Harrison, R. M., Beddows, D., O'Dowd, C., Jennings, S. G., Flentje, H., Weinhold, K., Meinhardt, F., Ries, L., and Kulmala, M.: Number size distributions and seasonality of submicron particles in Europe 2008–2009, Atmos. Chem. Phys., 11, 5505-5538, 10.5194/acp-11-5505-2011, 2011.

Bellouin, N., Quaas, J., Gryspeerdt, E., Kinne, S., Stier, P., Watson-Parris, D., Boucher, O., Carslaw, K. S., Christensen, M., Daniau, A. L., Dufresne, J. L., Feingold, G., Fiedler, S., Forster, P., Gettelman, A., Haywood, J. M., Lohmann, U., Malavelle, F., Mauritsen, T., McCoy, D. T., Myhre, G., Mulmenstadt, J., Neubauer, D., Possner, A., Rugenstein, M., Sato, Y., Schulz, M., Schwartz, S. E., Sourdeval, O., Storelvmo, T., Toll, V., Winker, D., and Stevens, B.: Bounding Global Aerosol Radiative Forcing of Climate Change, Rev. Geophys., 58, e2019RG000660, 10.1029/2019RG000660, 2020.

Bianchi, F., Kurten, T., Riva, M., Mohr, C., Rissanen, M. P., Roldin, P., Berndt, T., Crounse, J. D., Wennberg, P. O., Mentel, T. F., Wildt, J., Junninen, H., Jokinen, T., Kulmala, M., Worsnop, D. R., Thornton, J. A., Donahue, N., Kjaergaard, H. G., and Ehn, M.: Highly Oxygenated Organic Molecules (HOM) from Gas-Phase Autoxidation Involving Peroxy Radicals: A Key Contributor to Atmospheric Aerosol, Chem. Rev., 119, 3472-3509, 10.1021/acs.chemrev.8b00395, 2019.

Bianchi, F., Trostl, J., Junninen, H., Frege, C., Henne, S., Hoyle, C. R., Molteni, U., Herrmann, E., Adamov, A., Bukowiecki, N., Chen, X., Duplissy, J., Gysel, M., Hutterli, M., Kangasluoma, J., Kontkanen, J., Kurten, A., Manninen, H. E., Munch, S., Perakyla, O., Petaja, T., Rondo, L., Williamson, C., Weingartner, E., Curtius, J., Worsnop, D. R., Kulmala, M., Dommen, J., and Baltensperger, U.: New particle formation in the free troposphere: A question of chemistry and timing, Science, 352, 1109-1112, 10.1126/science.aad5456, 2016.

Boy, M., Karl, T., Turnipseed, A., Mauldin, R. L., Kosciuch, E., Greenberg, J., Rathbone, J., Smith, J., Held, A., Barsanti, K., Wehner, B., Bauer, S., Wiedensohler, A., Bonn, B., Kulmala, M., and Guenther, A.: New particle formation in the Front Range of the Colorado Rocky Mountains, Atmos. Chem. Phys., 8, 1577-1590, 10.5194/acp-8-1577-2008, 2008.

Carslaw, K. S.: Chapter 2 - Aerosol in the climate system, in: Aerosols and Climate, edited by: Carslaw, K. S., Elsevier, 9-52, https://doi.org/10.1016/B978-0-12-819766-0.00008-0, 2022.

Carslaw, K. S., Lee, L. A., Reddington, C. L., Pringle, K. J., Rap, A., Forster, P. M., Mann, G. W., Spracklen, D. V., Woodhouse, M. T., Regayre, L. A., and Pierce, J. R.: Large contribution of natural aerosols to uncertainty in indirect forcing, Nature, 503, 67-71, 10.1038/nature12674, 2013.

Deng, C. J., Fu, Y. Y., Dada, L., Yan, C., Cai, R. L., Yang, D. S., Zhou, Y., Yin, R. J., Lu, Y. Q., Li, X. X., Qiao, X. H., Fan, X. L., Nie, W., Kontkanen, J., Kangasluoma, J., Chu, B. W., Ding, A. J., Kerminen, V. M., Paasonen, P., Worsnop, D. R., Bianchi, F., Liu, Y. C., Zheng, J., Wang, L., Kulmala, M., and Jiang, J. K.: Seasonal Characteristics of New Particle Formation and Growth in Urban Beijing, Environ. Sci. Technol., 54, 8547-8557, 10.1021/acs.est.0c00808, 2020.

https://doi.org/10.5194/egusphere-2024-401
Preprint. Discussion started: 13 February 2024

Dunne, E. M., Gordon, H., Kurten, A., Almeida, J., Duplissy, J., Williamson, C., Ortega, I. K., Pringle, K. J., Adamov, A., Baltensperger, U., Barmet, P., Benduhn, F., Bianchi, F., Breitenlechner, M., Clarke, A., Curtius, J., Dommen, J., Donahue, N. M., Ehrhart, S., Flagan, R. C., Franchin, A., Guida, R., Hakala, J., Hansel, A., Heinritzi, M., Jokinen, T., Kangasluoma, J., Kirkby, J., Kulmala, M., Kupc, A., Lawler, M. J., Lehtipalo, K., Makhmutov, V., Mann, G., Mathot, S., Merikanto, J., Miettinen, P., Nenes, A., Onnela, A., Rap, A., Reddington, C. L. S., Riccobono, F., Richards, N. A. D., Rissanen, M. P., Rondo, L., Sarnela, N., Schobesberger, S., Sengupta, K., Simon, M., Sipilaa, M., Smith, J. N., Stozkhov, Y., Tome, A., Trostl, J., Wagner, P. E., Wimmer, D., Winkler, P. M., Worsnop, D. R., and Carslaw, K. S.: Global atmospheric particle formation from CERN CLOUD measurements, Science, 354, 1119-1124, 10.1126/science.aaf2649, 2016.

Ehn, M., Thornton, J. A., Kleist, E., Sipila, M., Junninen, H., Pullinen, I., Springer, M., Rubach, F., Tillmann, R., Lee, B., Lopez-Hilfiker, F., Andres, S., Acir, I. H., Rissanen, M., Jokinen, T., Schobesberger, S., Kangasluoma, J., Kontkanen, J., Nieminen, T., Kurten, T., Nielsen, L. B., Jorgensen, S., Kjaergaard, H. G., Canagaratna, M., Dal Maso, M., Berndt, T., Petaja, T., Wahner, A., Kerminen, V. M., Kulmala, M., Worsnop, D. R., Wildt, J., and Mentel, T. F.: A large source of low-volatility secondary organic aerosol, Nature, 506, 476-+, 10.1038/nature13032, 2014.

Emmons, L. K., Schwantes, R. H., Orlando, J. J., Tyndall, G., Kinnison, D., Lamarque, J. F., Marsh, D., Mills, M. J., Tilmes, S., Bardeen, C., Buchholz, R. R., Conley, A., Gettelman, A., Garcia, R., Simpson, I., Blake, D. R., Meinardi, S., and Pétron, G.: The Chemistry Mechanism in the Community Earth System Model Version 2 (CESM2), J. Adv. Model. Earth Sy., 12, 10.1029/2019ms001882, 2020.

Eyring, V., Bony, S., Meehl, G. A., Senior, C. A., Stevens, B., Stouffer, R. J., and Taylor, K. E.: Overview of the Coupled Model Intercomparison Project Phase 6 (CMIP6) experimental design and organization, Geosci. Model Dev., 9, 1937-1958, 10.5194/gmd-9-1937-2016, 2016.

Garmash, O., Rissanen, M. P., Pullinen, I., Schmitt, S., Kausiala, O., Tillmann, R., Zhao, D., Percival, C., Bannan, T. J., Priestley, M., Hallquist, Å. M., Kleist, E., Kiendler-Scharr, A., Hallquist, M., Berndt, T., McFiggans, G., Wildt, J., Mentel, T. F., and Ehn, M.: Multi-generation OH oxidation as a source for highly oxygenated organic molecules from aromatics, Atmos. Chem. Phys., 20, 515-537, 10.5194/acp-20-515-2020, 2020.

Gordon, H., Kirkby, J., Baltensperger, U., Bianchi, F., Breitenlechner, M., Curtius, J., Dias, A., Dommen, J., Donahue, N. M., Dunne, E. M., Duplissy, J., Ehrhart, S., Flagan, R. C., Frege, C., Fuchs, C., Hansel, A., Hoyle, C. R., Kulmala, M., Kurten, A., Lehtipalo, K., Makhmutov, V., Molteni, U., Rissanen, M. P., Stozkhov, Y., Trostl, J., Tsagkogeorgas, G., Wagner, R., Williamson, C., Wimmer, D., Winkler, P. M., Yan, C., and Carslaw, K. S.: Causes and importance of new particle formation in the present-day and preindustrial atmospheres, J. Geophys. Res.-Atmos., 122, 8739-8760, 10.1002/2017jd026844, 2017.

Gordon, H., Sengupta, K., Rap, A., Duplissy, J., Frege, C., Williamson, C., Heinritzi, M., Simon, M., Yan, C., Almeida, J., Trostl, J., Nieminen, T., Ortega, I. K., Wagner, R., Dunne, E. M., Adamov, A., Amorim, A., Bernhammer, A. K., Bianchi, F., Breitenlechner, M., Brilke, S., Chen, X. M., Craven, J. S., Dias, A., Ehrhart, S., Fischer, L., Flagan, R. C., Franchin, A., Fuchs, C., Guida, R., Hakala, J., Hoyle, C. R., Jokinen, T., Junninen, H., Kangasluoma, J., Kim, J., Kirkby, J., Krapf, M., Kurten, A., Laaksonen, A., Lehtipalo, K., Makhmutov, V., Mathot, S., Molteni, U., Monks, S. A., Onnela, A., Perakyla, O., Piel, F., Petaja, T., Praplanh, A. P., Pringle, K. J., Richards, N. A. D., Rissanen, M. P., Rondo, L., Sarnela, N., Schobesberger, S., Scott, C. E., Seinfeldo, J. H., Sharma, S., Sipila, M., Steiner, G., Stozhkov, Y., Stratmann, F., Tome, A., Virtanen, A., Vogel, A. L., Wagner, A. C., Wagner, P. E., Weingartner, E., Wimmer, D., Winkler, P. M., Ye, P. L., Zhang, X., Hansel, A., Dommen, J., Donahue, N. M., Worsnop, D. R., Baltensperger, U., Kulmala, M., Curtius, J., and Carslaw, K. S.: Reduced anthropogenic aerosol radiative forcing caused by biogenic new particle formation, P. Natl. Acad. Sci. USA, 113, 12053-12058, 10.1073/pnas.1602360113, 2016.

Guenther, A. B., Jiang, X., Heald, C. L., Sakulyanontvittaya, T., Duhl, T., Emmons, L. K., and Wang, X.: The Model of Emissions of Gases and Aerosols from Nature version 2.1 (MEGAN2.1): an extended and updated framework for modeling biogenic emissions, Geosci. Model Dev., 5, 1471-1492, 10.5194/gmd-5-1471-2012, 2012.

Jo, D. S., Hodzic, A., Emmons, L. K., Marais, E. A., Peng, Z., Nault, B. A., Hu, W., Campuzano-Jost, P., and Jimenez, J. L.: A simplified parameterization of isoprene-epoxydiol-derived secondary organic aerosol (IEPOX-SOA) for global chemistry and climate models: a case study with GEOS-Chem v11-02-rc, Geosci. Model Dev., 12, 2983-3000, 10.5194/gmd-12-2983-2019, 2019.

Jo, D. S., Hodzic, A., Emmons, L. K., Tilmes, S., Schwantes, R. H., Mills, M. J., Campuzano-Jost, P., Hu, W., Zaveri, R. A., Easter, R. C., Singh, B., Lu, Z., Schulz, C., Schneider, J., Shilling, J. E., Wisthaler, A., and Jimenez, J. L.: Future changes in

https://doi.org/10.5194/egusphere-2024-401
Preprint. Discussion started: 13 February 2024

isoprene-epoxydiol-derived secondary organic aerosol (IEPOX SOA) under the Shared Socioeconomic Pathways: the importance of physicochemical dependency, Atmos. Chem. Phys., 21, 3395-3425, 10.5194/acp-21-3395-2021, 2021.
Jokinen, T., Berndt, T., Makkonen, R., Kerminen, V. M., Junninen, H., Paasonen, P., Stratmann, F., Herrmann, H., Guenther, A. B., Worsnop, D. R., Kulmala, M., Ehn, M., and Sipila, M.: Production of extremely low volatile organic compounds from biogenic emissions: Measured yields and atmospheric implications, P. Natl. Acad. Sci. USA, 112, 7123-7128, 10.1073/pnas.1423977112, 2015.
Kerminen, V. M. and Kulmala, M.: Analytical formulae connecting the "real" and the "apparent" nucleation rate and the nuclei number concentration for atmospheric nucleation events, J. Atmos. Sci., 33, 609-622, 10.1016/s0021-8502(01)00194-x, 2002.
Kerminen, V. M., Chen, X. M., Vakkari, V., Petaja, T., Kulmala, M., and Bianchi, F.: Atmospheric new particle formation and growth: review of field observations, Environ. Res. Lett., 13, 10.1088/1748-9326/aadf3c, 2018.
Kirkby, J., Duplissy, J., Sengupta, K., Frege, C., Gordon, H., Williamson, C., Heinritzi, M., Simon, M., Yan, C., Almeida, J., Trostl, J., Nieminen, T., Ortega, I. K., Wagner, R., Adamov, A., Amorim, A., Bernhammer, A. K., Bianchi, F., Breitenlechner, M., Brilke, S., Chen, X. M., Craven, J., Dias, A., Ehrhart, S., Flagan, R. C., Franchin, A., Fuchs, C., Guida, R., Hakala, J., Hoyle, C. R., Jokinen, T., Junninen, H., Kangasluoma, J., Kim, J., Krapf, M., Kurten, A., Laaksonen, A., Lehtipalo, K., Makhmutov, V., Mathot, S., Molteni, U., Onnela, A., Perakyla, O., Piel, F., Petaja, T., Praplan, A. P., Pringle, K., Rap, A., Richards, N. A. D., Riipinen, I., Rissanen, M. P., Rondo, L., Sarnela, N., Schobesberger, S., Scott, C. E., Seinfeld, J. H., Sipila, M., Steiner, G., Stozhkov, Y., Stratmann, F., Tome, A., Virtanen, A., Vogel, A. L., Wagner, A. C., Wagner, P. E., Weingartner, E., Wimmer, D., Winkler, P. M., Ye, P. L., Zhang, X., Hansel, A., Dommen, J., Donahue, N. M., Worsnop, D. R., Baltensperger, U., Kulmala, M., Carslaw, K. S., and Curtius, J.: Ion-induced nucleation of pure biogenic particles, Nature, 533, 521-+, 10.1038/nature17953, 2016.
Kooperman, G. J., Pritchard, M. S., Ghan, S. J., Wang, M., Somerville, R. C. J., and Russell, L. M.: Constraining the influence of natural variability to improve estimates of global aerosol indirect effects in a nudged version of the Community Atmosphere Model 5, J. Geophys. Res.-Atmos.,, 117, 10.1029/2012jd018588, 2012.
Krapf, M., El Haddad, I., Bruns, Emily A., Molteni, U., Daellenbach, Kaspar R., Prévôt, André S. H., Baltensperger, U., and Dommen, J.: Labile Peroxides in Secondary Organic Aerosol, Chem, 1, 603-616, https://doi.org/10.1016/j.chempr.2016.09.007, 2016.
Kuang, C., McMurry, P. H., McCormick, A. V., and Eisele, F. L.: Dependence of nucleation rates on sulfuric acid vapor concentration in diverse atmospheric locations, J. Geophys. Res.-Atmos.,, 113, 10.1029/2007jd009253, 2008.
Kulmala, M.: How Particles Nucleate and Grow, Science, 302, 1000-1001, 10.1126/science.1090848, 2003.
Kulmala, M., Lehtinen, K. E. J., and Laaksonen, A.: Cluster activation theory as an explanation of the linear dependence between formation rate of 3nm particles and sulphuric acid concentration, Atmos. Chem. Phys., 6, 787-793, 10.5194/acp-6-787-2006, 2006.
Kulmala, M., Asmi, A., Lappalainen, H. K., Carslaw, K. S., Pöschl, U., Baltensperger, U., Hov, Ø., Brenquier, J. L., Pandis, S. N., Facchini, M. C., Hansson, H. C., Wiedensohler, A., and O'Dowd, C. D.: Introduction: European Integrated Project on Aerosol Cloud Climate and Air Quality interactions (EUCAARI) – integrating aerosol research from nano to global scales, Atmos. Chem. Phys., 9, 2825-2841, 10.5194/acp-9-2825-2009, 2009.
Lee, S., Shin, J. E., Yoon, R., Yoo, H., and Kim, S.: Annulation of O-silyl N,O-ketene acetals with alkynes for the synthesis of dihydropyridinones and its application in concise total synthesis of phenanthroindolizidine alkaloids, Front. Chem., 11, 1267422, 10.3389/fchem.2023.1267422, 2023.
Li, M., Liu, H., Geng, G., Hong, C., Liu, F., Song, Y., Tong, D., Zheng, B., Cui, H., Man, H., Zhang, Q., and He, K.: Anthropogenic emission inventories in China: a review, National Science Review, 4, 834-866, 10.1093/nsr/nwx150, 2017.
Liu, X., Ma, P. L., Wang, H., Tilmes, S., Singh, B., Easter, R. C., Ghan, S. J., and Rasch, P. J.: Description and evaluation of a new four-mode version of the Modal Aerosol Module (MAM4) within version 5.3 of the Community Atmosphere Model, Geosci. Model Dev., 9, 505-522, 10.5194/gmd-9-505-2016, 2016.
Liu, Y., Dong, X., Wang, M., Xu, R., Thornton, J. A., Shao, X., Emmons, L. K., Jo, D. S., Yue, M., and Shrivastava, M.: A Modeling Study of Global Distribution and Formation Pathways of Highly Oxygenated Organic Molecules Derived Secondary Organic Aerosols (HOMs-SOA) from MonoterpenesA Modeling Study of Global Distribution and Formation Pathways of Highly Oxygenated Organic Molecules Derived Secondary Organic Aerosols (HOMs-SOA) from Monoterpenes, J. Geophys. Res.-Atmos., (under review), 2024.

https://doi.org/10.5194/egusphere-2024-401
Preprint. Discussion started: 13 February 2024

Liu, Y., Dong, X., Emmons, L. K., Jo, D. S., Liu, Y., Shrivastava, M., Yue, M., Liang, Y., Song, Z., He, X., and Wang, M.: Exploring the Factors Controlling the Long-Term Trend (1988–2019) of Surface Organic Aerosols in the Continental United States by Simulations, J. Geophys. Res.-Atmos., 128, 10.1029/2022jd037935, 2023.

Luo, Z., Zhang, Y., Chen, W., Van Damme, M., Coheur, P. F., and Clarisse, L.: Estimating global ammonia (NH3) emissions based on IASI observations from 2008 to 2018, Atmos. Chem. Phys., 22, 10375-10388, 10.5194/acp-22-10375-2022, 2022.

Mann, G. W., Carslaw, K. S., Reddington, C. L., Pringle, K. J., Schulz, M., Asmi, A., Spracklen, D. V., Ridley, D. A., Woodhouse, M. T., Lee, L. A., Zhang, K., Ghan, S. J., Easter, R. C., Liu, X., Stier, P., Lee, Y. H., Adams, P. J., Tost, H., Lelieveld, J., Bauer, S. E., Tsigaridis, K., van Noije, T. P. C., Strunk, A., Vignati, E., Bellouin, N., Dalvi, M., Johnson, C. E., Bergman, T., Kokkola, H., von Salzen, K., Yu, F., Luo, G., Petzold, A., Heintzenberg, J., Clarke, A., Ogren, J. A., Gras, J., Baltensperger, U., Kaminski, U., Jennings, S. G., O'Dowd, C. D., Harrison, R. M., Beddows, D. C. S., Kulmala, M., Viisanen, Y., Ulevicius, V., Mihalopoulos, N., Zdimal, V., Fiebig, M., Hansson, H. C., Swietlicki, E., and Henzing, J. S.: Intercomparison and evaluation of global aerosol microphysical properties among AeroCom models of a range of complexity, Atmos. Chem. Phys., 14, 4679-4713, 10.5194/acp-14-4679-2014, 2014.

McMurry, P. H., Fink, M., Sakurai, H., Stolzenburg, M. R., Mauldin, R. L., Smith, J., Eisele, F., Moore, K., Sjostedt, S., Tanner, D., Huey, L. G., Nowak, J. B., Edgerton, E., and Voisin, D.: A criterion for new particle formation in the sulfur-rich Atlanta atmosphere, J. Geophys. Res.-Atmos., 110, 10.1029/2005jd005901, 2005.

Merikanto, J., Napari, I., Vehkamaki, H., Anttila, T., and Kulmala, M.: New parameterization of sulfuric acid-ammonia-water ternary nucleation rates at tropospheric conditions, J. Geophys. Res.-Atmos., 112, 10.1029/2006jd007977, 2007.

Merikanto, J., Spracklen, D. V., Mann, G. W., Pickering, S. J., and Carslaw, K. S.: Impact of nucleation on global CCN, Atmos. Chem. Phys., 9, 8601-8616, 10.5194/acp-9-8601-2009, 2009.

Mohr, C., Thornton, J. A., Heitto, A., Lopez-Hilfiker, F. D., Lutz, A., Riipinen, I., Hong, J., Donahue, N. M., Hallquist, M., Petaja, T., Kulmala, M., and Yli-Juuti, T.: Molecular identification of organic vapors driving atmospheric nanoparticle growth, Nat.Commun., 10, 10.1038/s41467-019-12473-2, 2019.

Molteni, U., Bianchi, F., Klein, F., El Haddad, I., Frege, C., Rossi, M. J., Dommen, J., and Baltensperger, U.: Formation of highly oxygenated organic molecules from aromatic compounds, Atmos. Chem. Phys., 18, 1909-1921, 10.5194/acp-18-1909-2018, 2018.

Paasonen, P., Nieminen, T., Asmi, E., Manninen, H. E., Petäjä, T., Plass-Dülmer, C., Flentje, H., Birmili, W., Wiedensohler, A., Hõrrak, U., Metzger, A., Hamed, A., Laaksonen, A., Facchini, M. C., Kerminen, V. M., and Kulmala, M.: On the roles of sulphuric acid and low-volatility organic vapours in the initial steps of atmospheric new particle formation, Atmos. Chem. Phys., 10, 11223-11242, 10.5194/acp-10-11223-2010, 2010.

Pierce, J. R. and Adams, P. J.: A Computationally Efficient Aerosol Nucleation/ Condensation Method: Pseudo-Steady-State Sulfuric Acid, Aerosol Sci. Technol., 43, 216-226, 10.1080/02786820802587896, 2009.

Pye, H. O. T., D'Ambro, E. L., Lee, B. H., Schobesberger, S., Takeuchi, M., Zhao, Y., Lopez-Hilfiker, F., Liu, J., Shilling, J. E., Xing, J., Mathur, R., Middlebrook, A. M., Liao, J., Welti, A., Graus, M., Warneke, C., de Gouw, J. A., Holloway, J. S., Ryerson, T. B., Pollack, I. B., and Thornton, J. A.: Anthropogenic enhancements to production of highly oxygenated molecules from autoxidation, P. Natl. Acad. Sci. USA, 116, 6641-6646, 10.1073/pnas.1810774116, 2019.

Reddington, C. L., Carslaw, K. S., Stier, P., Schutgens, N., Coe, H., Liu, D., Allan, J., Browse, J., Pringle, K. J., Lee, L. A., Yoshioka, M., Johnson, J. S., Regayre, L. A., Spracklen, D. V., Mann, G. W., Clarke, A., Hermann, M., Henning, S., Wex, H., Kristensen, T. B., Leaitch, W. R., Pöschl, U., Rose, D., Andreae, M. O., Schmale, J., Kondo, Y., Oshima, N., Schwarz, J. P., Nenes, A., Anderson, B., Roberts, G. C., Snider, J. R., Leck, C., Quinn, P. K., Chi, X., Ding, A., Jimenez, J. L., and Zhang, Q.: The Global Aerosol Synthesis and Science Project (GASSP): Measurements and Modeling to Reduce Uncertainty, Bull. Amer. Meteor. Soc., 98, 1857-1877, 10.1175/bams-d-15-00317.1, 2017.

Riccobono, F., Schobesberger, S., Scott, C. E., Dommen, J., Ortega, I. K., Rondo, L., Almeida, J., Amorim, A., Bianchi, F., Breitenlechner, M., David, A., Downard, A., Dunne, E. M., Duplissy, J., Ehrhart, S., Flagan, R. C., Franchin, A., Hansel, A., Junninen, H., Kajos, M., Keskinen, H., Kupc, A., Kurten, A., Kvashin, A. N., Laaksonen, A., Lehtipalo, K., Makhmutov, V., Mathot, S., Nieminen, T., Onnela, A., Petaja, T., Praplan, A. P., Santos, F. D., Schallhart, S., Seinfeld, J. H., Sipila, M., Spracklen, D. V., Stozhkov, Y., Stratmann, F., Tome, A., Tsagkogeorgas, G., Vaattovaara, P., Viisanen, Y., Vrtala, A., Wagner, P. E., Weingartner, E., Wex, H., Wimmer, D., Carslaw, K. S., Curtius, J., Donahue, N. M., Kirkby, J., Kulmala, M., Worsnop, D. R., and Baltensperger, U.: Oxidation Products of Biogenic Emissions Contribute to Nucleation of Atmospheric Particles, Science, 344, 717-721, 10.1126/science.1243527, 2014.

https://doi.org/10.5194/egusphere-2024-401
Preprint. Discussion started: 13 February 2024

Roldin, P., Ehn, M., Kurtén, T., Olenius, T., Rissanen, M. P., Sarnela, N., Elm, J., Rantala, P., Hao, L., Hyttinen, N., Heikkinen, L., Worsnop, D. R., Pichelstorfer, L., Xavier, C., Clusius, P., Öström, E., Petäjä, T., Kulmala, M., Vehkamäki, H., Virtanen, A., Riipinen, I., and Boy, M.: The role of highly oxygenated organic molecules in the Boreal aerosol-cloud-climate system, Nat.Commun., 10, 4370, 10.1038/s41467-019-12338-8, 2019.

Rosenfeld, D., Lohmann, U., Raga, G. B., O'Dowd, C. D., Kulmala, M., Fuzzi, S., Reissell, A., and Andreae, M. O.: Flood or Drought: How Do Aerosols Affect Precipitation?, Science, 321, 1309-1313, 10.1126/science.1160606, 2008.

Rosenfeld, D., Andreae, M. O., Asmi, A., Chin, M., de Leeuw, G., Donovan, D. P., Kahn, R., Kinne, S., Kivekäs, N., Kulmala, M., Lau, W., Schmidt, K. S., Suni, T., Wagner, T., Wild, M., and Quaas, J.: Global observations of aerosol-cloud-precipitation-climate interactions, Rev. Geophys., 52, 750-808, 10.1002/2013rg000441, 2014.

Scott, C. E., Rap, A., Spracklen, D. V., Forster, P. M., Carslaw, K. S., Mann, G. W., Pringle, K. J., Kivekäs, N., Kulmala, M., Lihavainen, H., and Tunved, P.: The direct and indirect radiative effects of biogenic secondary organic aerosol, Atmos. Chem. Phys., 14, 447-470, 10.5194/acp-14-447-2014, 2014.

Shiraiwa, M., Ueda, K., Pozzer, A., Lammel, G., Kampf, C. J., Fushimi, A., Enami, S., Arangio, A. M., Frohlich-Nowoisky, J., Fujitani, Y., Furuyama, A., Lakey, P. S. J., Lelieveld, J., Lucas, K., Morino, Y., Poschl, U., Takahama, S., Takami, A., Tong, H., Weber, B., Yoshino, A., and Sato, K.: Aerosol Health Effects from Molecular to Global Scales, Environ. Sci. Technol., 51, 13545-13567, 10.1021/acs.est.7b04417, 2017.

Sihto, S. L., Kulmala, M., Kerminen, V. M., Dal Maso, M., Petaja, T., Riipinen, I., Korhonen, H., Arnold, F., Janson, R., Boy, M., Laaksonen, A., and Lehtinen, K. E. J.: Atmospheric sulphuric acid and aerosol formation: implications from atmospheric measurements for nucleation and early growth mechanisms, Atmos. Chem. Phys., 6, 4079-4091, 10.5194/acp-6-4079-2006, 2006.

Spracklen, D. V., Carslaw, K. S., Kulmala, M., Kerminen, V. M., Mann, G. W., and Sihto, S. L.: The contribution of boundary layer nucleation events to total particle concentrations on regional and global scales, Atmos. Chem. Phys., 6, 5631-5648, 10.5194/acp-6-5631-2006, 2006.

Spracklen, D. V., Carslaw, K. S., Merikanto, J., Mann, G. W., Reddington, C. L., Pickering, S., Ogren, J. A., Andrews, E., Baltensperger, U., Weingartner, E., Boy, M., Kulmala, M., Laakso, L., Lihavainen, H., Kivekas, N., Komppula, M., Mihalopoulos, N., Kouvarakis, G., Jennings, S. G., O'Dowd, C., Birmili, W., Wiedensohler, A., Weller, R., Gras, J., Laj, P., Sellegri, K., Bonn, B., Krejci, R., Laaksonen, A., Hamed, A., Minikin, A., Harrison, R. M., Talbot, R., and Sun, J.: Explaining global surface aerosol number concentrations in terms of primary emissions and particle formation, Atmos. Chem. Phys., 10, 4775-4793, 10.5194/acp-10-4775-2010, 2010.

Stolzenburg, D., Simon, M., Ranjithkumar, A., Kurten, A., Lehtipalo, K., Gordon, H., Ehrhart, S., Finkenzeller, H., Pichelstorfer, L., Nieminen, T., He, X. C., Brilke, S., Xiao, M., Amorim, A., Baalbaki, R., Baccarini, A., Beck, L., Brakling, S., Murillo, L. C., Chen, D. X., Chu, B. W., Dada, L., Dias, A., Dommen, J., Duplissy, J., El Haddad, I., Fischer, L., Carracedo, L. G., Heinritzi, M., Kim, C., Koenig, T. K., Kong, W., Lamkaddam, H., Lee, C. P., Leiminger, M., Li, Z. J., Makhmutov, V., Manninen, H. E., Marie, G., Marten, R., Muller, T., Nie, W., Partoll, E., Petaja, T., Pfeifer, J., Philippov, M., Rissanen, M. P., Rorup, B., Schobesberger, S., Schuchmann, S., Shen, J. L., Sipila, M., Steiner, G., Stozhkov, Y., Tauber, C., Tham, Y. J., Tome, A., Vazquez-Pufleau, M., Wagner, A. C., Wang, M. Y., Wang, Y. H., Weber, S. K., Wimmer, D., Wlasits, P. J., Wu, Y. S., Ye, Q., Zauner-Wieczorek, M., Baltensperger, U., Carslaw, K. S., Curtius, J., Donahue, N. M., Flagan, R. C., Hansel, A., Kulmala, M., Lelieveld, J., Volkamer, R., Kirkby, J., and Winkler, P. M.: Enhanced growth rate of atmospheric particles from sulfuric acid, Atmos. Chem. Phys., 20, 7359-7372, 10.5194/acp-20-7359-2020, 2020.

Vehkamaki, H., Kulmala, M., Napari, I., Lehtinen, K. E. J., Timmreck, C., Noppel, M., and Laaksonen, A.: An improved parameterization for sulfuric acid-water nucleation rates for tropospheric and stratospheric conditions, J. Geophys. Res.-Atmos., 107, 10.1029/2002jd002184, 2002.

Wang, M. and Penner, J. E.: Aerosol indirect forcing in a global model with particle nucleation, Atmos. Chem. Phys., 9, 239-260, 10.5194/acp-9-239-2009, 2009.

Wang, M., Penner, J. E., and Liu, X.: Coupled IMPACT aerosol and NCAR CAM3 model: Evaluation of predicted aerosol number and size distribution, J. Geophys. Res.-Atmos.,, 114, 10.1029/2008jd010459, 2009.

Wang, S. N., Wu, R. R., Berndt, T., Ehn, M., and Wang, L. M.: Formation of Highly Oxidized Radicals and Multifunctional Products from the Atmospheric Oxidation of Alkylbenzenes, Environ. Sci. Technol., 51, 8442-8449, 10.1021/acs.est.7b02374, 2017.

https://doi.org/10.5194/egusphere-2024-401
Preprint. Discussion started: 13 February 2024

Wang, Y., Mehra, A., Krechmer, J. E., Yang, G., Hu, X., Lu, Y., Lambe, A., Canagaratna, M., Chen, J., Worsnop, D., Coe, H., and Wang, L.: Oxygenated products formed from OH-initiated reactions of trimethylbenzene: autoxidation and accretion, Atmos. Chem. Phys., 20, 9563-9579, 10.5194/acp-20-9563-2020, 2020.

Weber, J., Archer-Nicholls, S., Griffiths, P., Berndt, T., Jenkin, M., Gordon, H., Knote, C., and Archibald, A. T.: CRI-HOM: A novel chemical mechanism for simulating highly oxygenated organic molecules (HOMs) in global chemistry–aerosol–climate models, Atmos. Chem. Phys., 20, 10889-10910, 10.5194/acp-20-10889-2020, 2020.

Weber, R. J., Marti, J. J., McMurry, P. H., Eisele, F. L., Tanner, D. J., and Jefferson, A.: Measurements of new particle formation and ultrafine particle growth rates at a clean continental site, J. Geophys. Res.-Atmos.,, 102, 4375-4385, 10.1029/96jd03656, 1997.

Wendisch, M., Pöschl, U., Andreae, M. O., Machado, L. A. T., Albrecht, R., Schlager, H., Rosenfeld, D., Martin, S. T., Abdelmonem, A., Afchine, A., Araùjo, A. C., Artaxo, P., Aufmhoff, H., Barbosa, H. M. J., Borrmann, S., Braga, R., Buchholz, B., Cecchini, M. A., Costa, A., Curtius, J., Dollner, M., Dorf, M., Dreiling, V., Ebert, V., Ehrlich, A., Ewald, F., Fisch, G., Fix, A., Frank, F., Fütterer, D., Heckl, C., Heidelberg, F., Hüneke, T., Jäkel, E., Järvinen, E., Jurkat, T., Kanter, S., Kästner, U., Kenntner, M., Kesselmeier, J., Klimach, T., Knecht, M., Kohl, R., Kölling, T., Krämer, M., Krüger, M., Krisna, T. C., Lavric, J. V., Longo, K., Mahnke, C., Manzi, A. O., Mayer, B., Mertes, S., Minikin, A., Molleker, S., Münch, S., Nillius, B., Pfeilsticker, K., Pöhlker, C., Roiger, A., Rose, D., Rosenow, D., Sauer, D., Schnaiter, M., Schneider, J., Schulz, C., de Souza, R. A. F., Spanu, A., Stock, P., Vila, D., Voigt, C., Walser, A., Walter, D., Weigel, R., Weinzierl, B., Werner, F., Yamasoe, M. A., Ziereis, H., Zinner, T., and Zöger, M.: ACRIDICON–CHUVA Campaign: Studying Tropical Deep Convective Clouds and Precipitation over Amazonia Using the New German Research Aircraft HALO, B. Am. Meteorol. Soc., 97, 1885-1908, https://doi.org/10.1175/BAMS-D-14-00255.1, 2016.

Xu, L., Pye, H. O. T., He, J., Chen, Y., Murphy, B. N., and Ng, N. L.: Experimental and model estimates of the contributions from biogenic monoterpenes and sesquiterpenes to secondary organic aerosol in the southeastern United States, Atmos. Chem. Phys., 18, 12613-12637, 10.5194/acp-18-12613-2018, 2018.

Xu, R. C., Thornton, J. A., Lee, B., Zhang, Y. X., Jaegle, L., Lopez-Hilfiker, F. D., Rantala, P., and Petaja, T.: Global simulations of monoterpene-derived peroxy radical fates and the distributions of highly oxygenated organic molecules (HOMs) and accretion products, Atmos. Chem. Phys., 22, 5477-5494, 10.5194/acp-22-5477-2022, 2022.

Yue, M., Dong, X., Wang, M., Emmons, L. K., Liang, Y., Tong, D., Liu, Y., and Liu, Y.: Modeling the Air Pollution and Aerosol-PBL Interactions Over China Using a Variable-Resolution Global Model, J. Geophys. Res.-Atmos.,, 128, 10.1029/2023jd039130, 2023.

Zaveri, R. A., Easter, R. C., Singh, B., Wang, H., Lu, Z., Tilmes, S., Emmons, L. K., Vitt, F., Zhang, R., Liu, X., Ghan, S. J., and Rasch, P. J.: Development and Evaluation of Chemistry-Aerosol-Climate Model CAM5-Chem-MAM7-MOSAIC: Global Atmospheric Distribution and Radiative Effects of Nitrate Aerosol, J Adv Model Earth Syst, 13, e2020MS002346, 10.1029/2020MS002346, 2021.

Zawadowicz, M. A., Lee, B. H., Shrivastava, M., Zelenyuk, A., Zaveri, R. A., Flynn, C., Thornton, J. A., and Shilling, J. E.: Photolysis Controls Atmospheric Budgets of Biogenic Secondary Organic Aerosol, Environ. Sci. Technol., 54, 3861-3870, 10.1021/acs.est.9b07051, 2020.

Zheng, J., Zhang, L., Che, W., Zheng, Z., and Yin, S.: A highly resolved temporal and spatial air pollutant emission inventory for the Pearl River Delta region, China and its uncertainty assessment, Atmos. Environ., 43, 5112-5122, https://doi.org/10.1016/j.atmosenv.2009.04.060, 2009.

Zhou, Y., Zhao, Y., Mao, P., Zhang, Q., Zhang, J., Qiu, L., and Yang, Y.: Development of a high-resolution emission inventory and its evaluation and application through air quality modeling for Jiangsu Province, China, Atmos. Chem. Phys., 17, 211-233, 10.5194/acp-17-211-2017, 2017.

Zhu, J. and Penner, J. E.: Global Modeling of Secondary Organic Aerosol With Organic Nucleation, J. Geophys. Res.-Atmos.,, 124, 8260-8286, 10.1029/2019jd030414, 2019.

Zhu, J. L., Penner, J. E., Yu, F. Q., Sillman, S., Andreae, M. O., and Coe, H.: Decrease in radiative forcing by organic aerosol nucleation, climate, and land use change, Nat.Commun., 10, 10.1038/s41467-019-08407-7, 2019.